

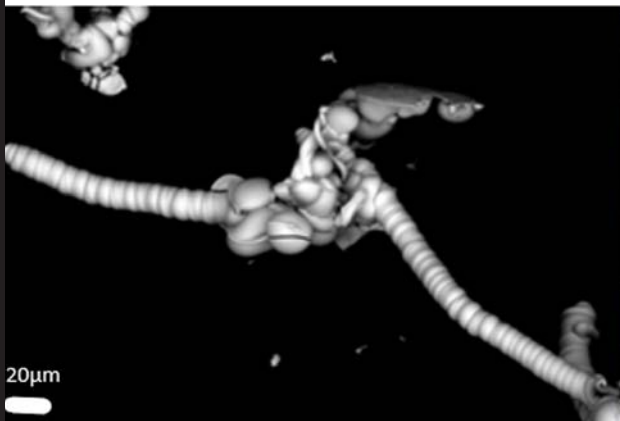
Seminarios de la Sociedad Española de Mineralogía

13

XXXVI Reunión de la Sociedad Española de Mineralogía

Crystallization under Extreme Conditions

Oviedo - Asturias (Spain)
July 4, 2017



Editores:
Amalia Jiménez
Manuel Prieto
Ángeles Fernández-González



www.ehu.es/sem

Seminarios de la Sociedad Española de Mineralogía

Volumen 13

Crystallization Under Extreme Conditions

Seminario celebrado en
Universidad de Oviedo, Edificio Histórico
July 4, 2017

Editores:
Amalia Jiménez
Manuel Prieto
Ángeles Fernández-González



Figure on the left: Biomorph of barium and silica carbonate. Purely inorganic structures that mimic the forms of primitive organisms and the textures of biominerals (García-Ruiz, J.M. 2017, Seminarios SEM 2017).

Figure on the right: Acicular gypsum crystals growing upwards from a streambed of an acidic mine effluent (field of view ~ 5 cm) (Sanchez-España, J. 2017, Seminarios SEM, 2017)



**Seminarios de la Sociedad de Española
de Mineralogía**

© Sociedad Española de Mineralogía
Museo Geominero del Instituto Geológico
y Minero de España
c/ Calle de Ríos Rosas, 23
28003 Madrid

<http://www.ehu.es/sem>
sem@ehu.es

Editores

Amalia Jiménez
Manuel Prieto
Ángeles Fernández-González

Diseño y maquetación

Soma Dixital, S.L.

Impresión

Lugami Artes Gráficas, S.L.

Depósito legal

CA-602-2004

ISSN

1698-5478

Impreso en España - Printed in Spain (2017)

Foreword

Crystallization is a natural process that occurs in environments with very different conditions in the earth's crust. During the last decades, the scientific community has discovered that under extreme conditions the crystallization of minerals and other substances can serve as an example to understand aspects as important as the origin of life, the geology of Mars or the development of new engineering materials. The aim of this volume is to bring together the experts and early-stage researchers interested in the wide range of phenomena associated with mineral growth, dissolution, and replacement processes in extreme conditions, such as extremely acidic or alkaline natural and anthropogenic scenarios and confined environments.

In this issue, Juan Manuel Garcia-Ruiz shows different examples of mineral self-assembled patterns formed under extreme geochemical conditions, which are compatible with life and prebiotic chemistry. He brings us a collection of studies on morphological behavior of precipitates and demonstrates that inorganic processes provide shapes reminiscent of primitive living organisms.

The contribution by Françoise Guyot and Aurore Gorlas shows the growth of minerals induced and/or controlled by microorganisms living in hydrothermal chimneys into the ocean. These authors discuss the sequence of nucleation and growth observed in experiments specifically designed to study the biomineralization in such extreme environments.

In the next chapter, Javier Sanchez España provides a comprehensive review of the mineral phases formed in acidic waters. This study involves the chemical conditions leading to their formation (precipitation or crystallization) of the most common mineral, such as sulphates, oxy-hydroxysulphates and sulphides covering a wide range in size (from nano-particles to large crystals) and crystalline order (from nearly amorphous to highly crystalline).

The final chapter by Alejandro Fernandez-Martinez is interested in nucleation and crystallization processes in confined spaces. Studies on complex multi-stage nucleation pathways point out the similarities between processes involved in natural and engineering cements. This author proposes that further research to develop a future generation of 'cement' products inspired by nature is necessary.

These chapters compile the issues presented by the invited speakers at the workshop on "Crystallization under extreme conditions" held prior to the XXXVI Reunion of SEM in Oviedo (5-7 July, 2017). This volume would not have been possible without the collaboration and enthusiasm of the authors, who responded immediately to our request to participate in the workshop. Our sincere acknowledgement to expertise that kindly submitted their contributions before the workshop. We would like to express a special thanks to the institutions, the University of Oviedo, the city council of Oviedo and the Government of the Principality of Asturias, and eight sponsors (ALS, Asturiana de Zinc, Chemlabor, Dismed, Fundacion Caja Rural, Insertec, Minersa and PanAnalytical) that have provided logistics and generous financial support to the organization of this workshop. All of them have made possible the publication of this volume and its distribution to all SEM members.

Amalia Jiménez Bautista
Manuel Prieto Rubio

Index / Índice

- 05** Mineral Self-assembly Under Extreme Geochemical Conditions and its Relevance to Primitive Life Detection
Juan Manuel García-Ruiz
- 13** Biomineralization in hydrothermal systems
Francois Guyot & Aurore Gorlas
- 15** Crystallization in acidic media: from nanoparticles to macrocrystals
Javier Sánchez España
- 35** Multi-step crystallization pathways in natural and engineered cements
Alejandro Fernandez-Martinez

Mineral self-assembly under extreme geochemical conditions and its relevance to primitive life detection

/ Juan Manuel García-Ruiz

Laboratorio de Estudios Cristalográficos, IACT (CSIC-UGR), Av. de las Palmeras 4, E-18100 Armilla, Granada, Spain

1. Introduction

The detection of primitive life remnants in the older terrestrial rocks is an important research subject to set the timing of life on our planet (*Schopf, 1983*). As space technology advances, it will also be an essential research to know if our sister planet Mars is or not devoid of life, i.e. to know if life is or not a single unique event in the Universe (*McKay et al., 1996*). Unfortunately, identification of actual remnants of living forms from purely inorganic mineral microstructures sharing morphological and chemical properties is a formidable challenge (*van Zuilen 2002; Grotzinger & Knoll, 1999*). Nowadays, the identification of oldest remnants of life in Archean rocks mostly relies on morphology. Certainly, there are other analytical techniques such as isotopic analysis, high resolution electron microscopies to reveal the intimate structure of carbonaceous materials, and chemical identification of molecules unequivocally linked to life (molecular fossils), but all they have problems of consistency. Thus, morphological studies are critical for life detection. However, as we have claimed in 2002, morphology itself is not a reliable tool for the unambiguous identification of primitive life remnants (*García-Ruiz et al., 2002*). More precisely, the claim is that morphology does not contain definitive information on morphogenesis. This assertion could come as a shock to biologists who used to identify fossils by their morphologies, so different that the morphology of minerals and rocks. However, it should be remembered that what we use to identify fossils of ammonites, trilobites or dinosaurs as remnants of life is not morphology but comparative anatomy introduced by Cuvier in XIX century. The problem when looking for oldest remnants of life is that they are tiny and simple pieces of rocks. In this case, we are dealing with simple shapes, poor or no compartmentalization at all, namely microspheres, microrods, tubules, septated tubular shapes, simple helicoids, discoid shapes, and a few other simple shapes. Therefore it is impossible to apply comparative anatomy to these putative fossils. Thus, when identifying the physical structures of possible oldest remnants of life in this planet or primitive life in extraterrestrial bodies, we have nothing else than morphology. This made the unambiguous differentiation of actual life remnants from inorganic biomimetic counterparts a task that must be performed with caution.

The ability of inorganic precipitation processes to produce the characteristic shapes of life i.e. shapes described by fractal branching and continuous curvature, cannot be today considered an astonishing property of matter (*Fig. 1*). Structures with non-crystallographic morphologies mimicking primitive living organisms can be readily obtained under conditions mimicking the plausible geochemistry of a lifeless planet. There are different chemical reactions and physical precipitation/dissolution phenomena leading to micro- and macro-patterning strongly resembling biological organisms in both, shape

and scale. As said above, the community of micropaleontologists accepts nowadays that morphology alone does not inform on biogenicity. The same must be also accepted for those colleagues flattened by laboratory structures made in the laboratory strongly mimicking the shape of primitive life forms. Therefore, any comparison between microfossils or putative microfossils with abiotic biomimetic mineral structures must focus on detailed textures and decoration beyond morphology, as well as on inorganic morphogenesis. Any relevant study to life detection must consider and offer, at least, the following information:

- 1) A demonstration that the geochemical scenario of the rocks embedding the microfossils or putative microfossils is compatible with the chemical reactions invoked to explain the formation of the proposed abiotic structures.
- 2) A comparative study not only of the shape but also of the "decoration" of both abiotic model and putative microfossils.
- 3) A statistical study of the size and size distribution of the community of microstructures.
- 4) A morphogenetic explanation of the mechanism of formation of the complex abiotic structures.

The symmetry of natural shapes

(classical thought)

The realm of the crystal

Inorganic symmetry

Polyhedral, faceted shapes

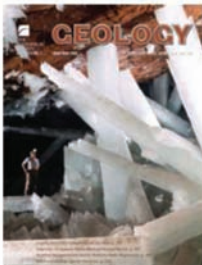
Deterministic angles

Forbidden symmetry operators

$$35 G^3_0 \subset K$$

$$A_{\gamma\gamma} = \text{minimum}$$

Shapes controlled by intimate ordered structures



The realm of life

Organic symmetry

Sinuous shapes

Continuous curvature

Unrestricted symmetry

$$\infty G^3_0 \not\subset K$$

$$A_{\gamma\gamma} > \text{minimum}$$

Shapes uncontrolled by intimate internal structure



Fig. 1. The existence of a sharp boundary dividing biology the realm of biology and sensuality and the realm of minerals and cold rationality has pervaded the landscape of science, arts, and philosophy for centuries. Crystals and crystallographic theories have played a major role in the intellectual construction of that false boundary.

Unfortunately, while there are hundreds of studies to analyze the morphology of fossil microstructures from the point of view of biology, there are very few studies devoted to exploring the formation of complex biomimetic morphologies by inorganic mineral precipitation (García-Ruiz, 1999; Brasier et al., 2006; Carnerup et al., 2006; Nakouzi & Steinbock, 2016). The morphological behavior of inorganic precipitation systems can be classified into three major groups (see Fig. 2). The first one includes all mineral objects in which pattern formation is controlled by the crystal structure of the precipitating mineral phase. This group is the classical domain of mineral morphology (see for instance the view offered by the Dana System of Mineralogy or the book of Sunagawa, 2005). It comprises single faceted crystals, twins, ordered dendrites and dendrites were forming when mass transport governs the formation of the pattern. For many years, this group has

been identified with the inorganic world, and it is usually assumed that those natural precipitates displaying well-defined geometry with non-crystallographic symmetry are generated under biological control. In addition to this standard type of mineral patterns, there are two other types, which do not fulfill that "rule." In the first one, the morphology of the precipitates is mainly controlled by the properties of a matrix (in some cases, ordered at the mesoscopic scale) and by osmotic forces working as the driving force for morphogenesis. The most classical organic but abiotic example is provided by the bilayers made of electrically neutral lipids, which exhibit phase transitions and instabilities leading from spherical and ellipsoidal shapes to more complicated patterns. Inorganic examples of this type of materials can be found, but the one I consider most geochemically plausible is obtained when carbonate precipitates at basic pH in silica-rich environ-

Inorganic biomimetic mineral patterns

Shape controlled by 3D crystal structure

- Additives adhering preferentially on crystalline faces
- Mesocrystals
- Spherulites
- Competitive crystal growth

Shape controlled by 2D crystal structure (The template way, top-down approach)

- Liquid crystals
- Crystallization on preexisting 2D surfaces
- Functionalized self-assembled monolayers
- Micelles, by-layers and colloidal structured surfaces

Shape controlled by transport and chemical reactions

Self-Organized bottom-up approach

- Diffusion–reaction patterns, such as Liesegang's precipitation.
- Dissipative structures
- Silica biomorphs
- Chaotic mixing of fluids,
- Fractal viscous fingering
- Diffusion limited aggregation
- Chemical gardens
- Self-propagating particles

Fig. 2. The morphological behavior of mineral-base structures is much richer than currently thought. Beyond classical point symmetry groups, there are three different classes of phenomena leading to self-organized and self-assembled materials mimicking the geometry and symmetry of life.

ments. The third group includes all the inorganic aggregates (composed of crystals, molecules, atoms or their clusters) in which the morphogenetic process is mainly controlled by the fluid structures in their growth environment. They are in fact the mineral decoration of these fluid structures, which turn out to be triggered by physical and chemical instabilities. The requirement for the material record of such non-equilibrium ordered patterns is that the kinetics of the precipitation must be faster than the kinetics of pattern formation in the fluid. In consequence, it is expected that this third kind of pattern will form at a very high supersaturation in a precipitating system working far from equilibrium pattern. There are two examples that illustrate very beautifully this kind of pattern. One is the case of manganese and iron oxide dendrites formed by the decoration of Saffman-Taylor interfaces, which display shapes with symmetry properties that are unconstrained by crystallographic restrictions. A second example is the case of chemical gardens, which are tubular precipitates forming by a complex interplay of osmosis, buoyancy and chemical reaction far from equilibrium (Glaab *et al.*, 2012).

2. Minerals Under Extreme Geochemical Conditions

I will discuss in detail in my lecture the above classification of complex mineral self-assembled patterns forming under extreme geochemical conditions compatible with life and prebiotic chemistry. Within this review, I will pay special attention to the following geochemical mineral structures that are relevant to life detection studies:

The chemical coupling of silica with carbonate at high pH that yields complex self-organized biomimetic shapes.

It has been shown that the chemical coupling of silica - an ubiquitous mineral in the Earth crust- with carbonates creates abiotic, purely inorganic, self-assembled

structures made of millions of nanocrystals building textures of high complexity and showing morphologies with continuous non-crystallographic curvature (García-Ruiz *et al.*, 2002 and 2003). I will review recent studies on the biomimetic effect of silica on carbonate precipitation under alkaline conditions and the geochemical plausibility of these self-organized mineral processes.

The co-precipitation of silica and metal oxides in the form tubular structures

The reaction between a soluble metal salt and soluble alkaline silicate is known to provoke a chemical precipitate with unusual morphological properties known as silica gardens (Kellermeier *et al.*, 2013). According to the membrane osmotic model, tubules in silicate gardens are produced by the injection of a jet of metal solution into the silicate solution when the membrane cracks as an effect of the internal osmotic pressure at the interface between the two fluids, a fast kinetic precipitation of a metal silicate hydrate occurs and the growth front and the interface becomes materially recorded. In the called silica gardens, the sodium silicate solution is a viscous fluid in which mass convection transport exists and therefore turbulent patterns are created and sometimes destroyed by gravity. It has been shown that these structures can be made under geochemical conditions (García-Ruiz *et al.*, 2017) and it is worth to discuss to which extent this claim can be extrapolated to Hadean and Archean times. I will also discuss how relevant these structures have been in the catalysis of prebiotic chemical reactions (Barge *et al.*, 2015; Saladino *et al.*, 2016).

The formation of stromatolite-like structures (Altermann 2004)

Stromatolites are very interesting for two different reasons. The first one is that they are the oldest putative signatures of life on the Earth, and the second that they are a good example of the difficulty encountered in decoding the genetic mechanism of natural structures through the study of their morphological features.

Stromatolites are banded mineral structures made up of calcium carbonates that show a certain degree of corrugation. It is clear that contemporarily, they are the results of life activity, as demonstrated by the examples found in Shark Bay in Australia and many other examples elsewhere. Similar structures have been found in very old Archean rocks and they have been considered proof of bacterial activity at those early times (*Allwood et al., 2006*). However, serious doubts have arisen regarding such a straightforward interpretation (*Grotzinger & Knoll 1999*). Stromatolites, like other corrugate patterns, can be considered (at least within a certain range of scale) fractal structures and they can be characterized by a given fractal dimension.

The stromatolitic structure is paradigmatic case for the misuse of fractal geometry in natural morphogenesis studies. The recent introduction of fractal geometry to measure biological and geological patterns up to now described as just complicated or intricate patterns is a new and powerful tool in modern Natural History studies. Unfortunately, in many cases the meaning of these fractal studies has been extrapolated beyond reasonable limits for a geometrical tool. Considering Euclidean shapes, could one infer a tree-type genetic mechanism for a tennis ball because they scale with a power of 3 like the shape of an orange does? The answer is obviously no because geometry does not contain in itself genetic information. Exactly the same occurs when comparing fractal shapes, with the tenuous (but important) difference that the power is usually a fractional number. Even in those serendipitous cases where the geometrical study yields a fractal dimension characteristic of a well-known physical mechanism such as diffusion limited aggregation (DLA), the problem can only be considered closed by a physicist, who arrives at the conclusion that a Laplacian-type mechanism must be involved in the generation of the structure. However, for scientists of Natural History it then starts to be a real pro-

blem, because Saffman-Taylor instability, diffusion controlled accretion phenomena and electrical conduction all share the same Laplacian mechanism. It is of the utmost importance to select among these when explaining the origin of biological or geological structures.

The formation of fractal dendrites of iron and manganese.

This group the well-known manganese and iron oxide dendrites (usually called pyrolusite dendrites) are unique in the emulation or fossil superior plants. They are non-crystallographic dendrites reminiscent of fern leaves, which exhibit fractal properties, as do fern leaves. These amazing forms, with a fractal dimension close to the golden number ($D_f = 1,70$) or diffusion limited aggregation can be observed in most Natural History museums and many mineral stores. However, when observed in the field, these amorphous oxides and oxyhydroxides exhibit many other form -always non-crystallographic ones- within a wide range of fractal dimensions. The formation of all these shapes can be explained as the result of a viscous fingering process. This process is triggered by Saffman-Taylor instabilities, which form when a low viscosity fluid pushes another one of higher viscosity. When slurries of dissolved manganese and/or iron II entrapped in rocks (particularly inside cracks and sedimentary laminations) is invaded and pushed by an oxygen-rich fluid. All these fractal forms are easily obtained, as has been experimentally demonstrated (*Fig. 3*). An alternative explanation based on a DLA-type mechanism has been also proposed.

Pyrite trails.

Tyler & Barghoorn, (1963) first reported these bizarre but rather common microstructures in Precambrian rocks made of pyrite grains with appendages. *Knoll & Barghoorn, (1974)* and other groups later studied them in detail. At least, four different types of pyrite trails in cherts in Precambrian and also in Archean rocks have been described. The

formation of these pyrite trails is still unknown. Revealing their origin could yield very interesting and novel information about the physicochemical conditions in the primitive Earth, and for the Proterozoic samples, also precious information either on the ecosystem or the taphonomy of primitive living organisms.

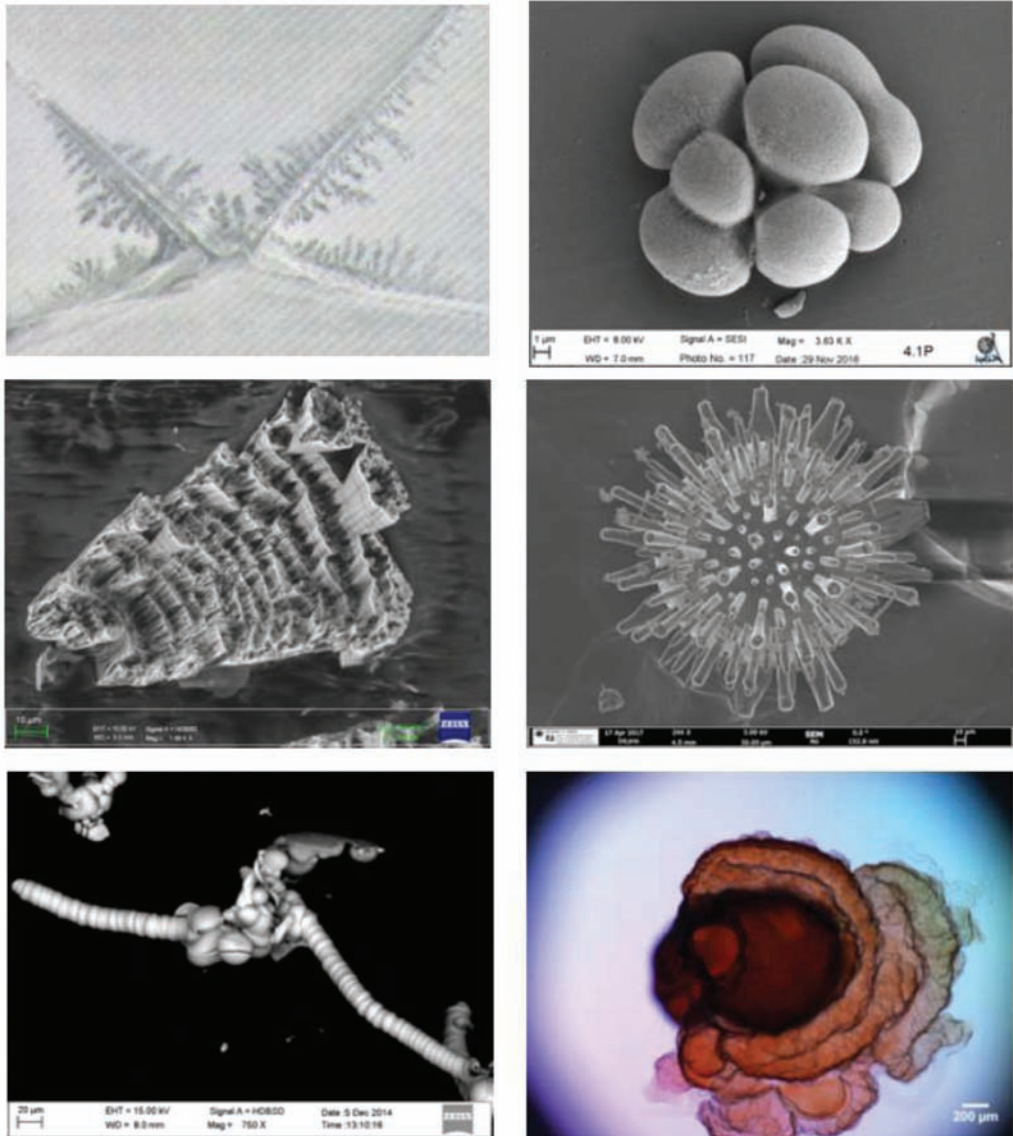


Fig. 3. Several examples of self-organized biomimetic structures. All pictures are from the lab's author.

Globular and embryo-like structures.

Polymeric compounds have been shown to induce splitting of the ends of elongated single crystals. These have been shown for the case of barium, strontium and calcium carbonate but also for calcium phosphates (*Kniep & Simon (2007)*). The continuous splitting leads the formation of dendrites with non-crystallographic branching that ends into random globular structures or embryo like cell partition (*Yin et al., 2007*).

Calcite single crystals with non-singular faces.

The ability of bacteria to induce distinctive features in the morphology and crystal arrangement of CaCO_3 precipitates has been widely reported. The subject is of great importance in the interpretation of limestone petrogenesis and a huge literature on field and laboratory studies has been published (*Buczynski & Chafetz, 1991*). The catalogue of forms included crystal bundles, rod-shaped crystals, dumbbell-shaped crystal aggregates, barrel-like, comb-like and brush-like forms (*Fig. 3*). There is no doubt that these bizarre habits of calcium carbonate occur linked to bacterial activity. In fact, they can be also observed in mineralized tissues of higher organisms, as they appear, for instance in eggshells, exoskeletons and otoliths. When looking in detail for the origin of these forms, it is clear that they arise because of the interaction of calcite and aragonite crystal faces with biological macromolecules. I will discuss how prebiotic chemical compounds and silica are able to mimic exactly the textural and morphological features of biological induced calcium carbonate precipitation.

Acknowledgments

This study has been supported by the Ministerio de Economía y Competitividad of Spain through the project CGL2016-78971-P.

References

- Allwood, A. C., Walter, M. R., Kamber, B. S., Marshall, C. P., & Burch, I. W. (2006) Stromatolite reef from the Early Archaean era of Australia. Nature, 441(7094), 714-718.*
- Altermann, W. (2004) Precambrian stromatolites: problems in definition, classification, morphology and stratigraphy, In: P.G. Eriksson, W. Altermann, D.R. Nelson, W.U. Mueller & O. Catuneanu (eds.) The Precambrian Earth: tempos and events, Developments in Precambrian Geology 12, 564-574.*
- Barge, L. M., Cardoso, S. S., Cartwright, J. H., Cooper, G. J., Cronin, L., De Wit, A., ... & Jones, D. E. (2015) From chemical gardens to chemobionics. Chemical reviews, 115(16), 8652-8703.*
- Brasier, M., McLoughlin, N., Green, O. and Wacey, D. (2006) A fresh look at the fossil evidence for early Archaean cellular life. Phil. Trans. R. Soc. B, 361, 887-902.*
- Buczynski, C. & Chafetz, H.S. (1991) Habit of bacterially induced precipitates of calcium carbonate and the influence of medium viscosity on mineralogy. J. Sediment. Petrol. 61, 226-233.*
- Carnerup, A. M.; Christy, A. G.; Garcia-Ruiz, J. M.; Hyde, S. T.; Larsson, A. K. (2006) The Record of Early Life: In search of biosignatures. In Life as We Know It, Seckbach, J., Ed. Springer Netherlands. 10, 237-258.*
- García-Ruiz, J. M. (1999) Morphological behavior of inorganic precipitation systems. In Instruments, Methods, and Missions for Astrobiology II, Hoover, R. B., Ed. Proceedings of SPIE: 1999; 3755, 74-82.*
- García Ruiz, J. M., Carnerup, A., Christy, A. G., Welham, N. J., & Hyde, S. T. (2002) Morphology: an ambiguous indicator of biogenicity. Astrobiology, 2(3), 353-369.*
- García-Ruiz, J. M., Hyde, S. T., Carnerup, A. M., Christy, A. G., Van Kranendonk, M. J., & Welham, N. J. (2003) Self-assembled silica-carbonate structures and detection of ancient microfossils. Science, 302(5648), 1194-1197.*

- García-Ruiz, J. M., Nakouzi, E., Kotopoulou, E., Tamborrino, L., & Steinbock, O. (2017) Biomimetic mineral self-organization from silica-rich spring waters. *Science Advances*, 3(3), e1602285.
- Glaab, F., Kellermeier, M., Kunz, W., Morallon, E., & García-Ruiz, J. M. (2012) Formation and Evolution of Chemical Gradients and Potential Differences Across Self-Assembling Inorganic Membranes. *Angewandte Chemie*, 124(18), 4393-4397.
- Grotzinger, J. P., & Knoll, A. H. (1999). Stromatolites in Precambrian carbonates: evolutionary mileposts or environmental dipsticks?. *Annual review of earth and planetary sciences*, 27(1), 313-358.
- Kellermeier, M., Glaab, F., Melero-García, E. & García-Ruiz, J. M. (2013) Experimental techniques for the growth and characterization of silica biomorphs and silica gardens in *Methods in Enzymology*, 532 of *Research Methods in Biomineralization Science*, (J. J. De Yoreo, Ed., Academic Press,) 225–256.
- Knoll, A. H., & Barghoorn, E. S. (1974) Ambient pyrite in Precambrian chert: new evidence and a theory. *Proceedings of the National Academy of Sciences*, 71(6), 2329-2331.
- Kniep, R., & Simon, P. (2007) Fluorapatite-gelatin-nanocomposites: self-organized morphogenesis, real structure and relations to natural hard materials. *Biomineralization I*, 73-125.
- McKay D. S., Gibson, E. K. Jr., Thomas-keprta K.L., Vali, H., Romanek, C.S., Clemett S. J., Chillier, X.D.F., Maechling, C.R., & Zare, N.R (1996) "Search for past life on Mars: Possible relict biogenic activity in Martian meteorite ALH84001. *Science* 273, 924-930.
- Nakouzi, E. & Steinbock, O. (2016) Self-organization in precipitation reactions far from the equilibrium. *Science Advances* 2, e1601144.
- Saladino, R., Botta, G., Bizzarri, B.M., Di Mauro, E. & García-Ruiz, J. M. (2016) A global scale scenario for prebiotic chemistry: Silica-based self-assembled mineral structures and formamide. *Biochemistry* 55, 2806–2811
- Schopf, W. (Ed)., (1983) *Earth's Earliest Biosphere*, Princeton University Press, Princeton, New Jersey, 543 pp.
- Sunagawa, I. (2005) *Growth, Morphology, and Perfection*. Cambridge University Press. 295 pp.
- Tyler, S. A., & Barghoorn, E. S. (1963). Ambient pyrite grains in Precambrian cherts. *American Journal of Science*, 261(5), 424-432.
- Van Zuilen, M. A., Lepland, A. & Arrhenius, G. (2002) Reassessing the evidence for the earliest traces of life. *Nature* 418, 627-630.
- Yin, L., Zhu, M., Knoll, A. H., Yuan, X., Zhang, J., & Hu, J. (2007). Doushantuo embryos preserved inside diapause egg cysts. *Nature*, 446(7136), 661-663.

Biom mineralization in hydrothermal systems

/ Francois Guyot (1) / Aurore Gorlas (2)

(1) IMPMC. Museum National d'Histoire Naturelle, Paris, France

(2) Laboratoire de Biologie Cellulaire des Archaea, Université Paris Sud, Orsay, France

Due to heat production in the bulk Earth, temperature increases with depth. Convection cells of water between the surface and the Earth's interior remove internal heat thus generating hot aqueous fluids which can reach temperatures of up to 400°C. These high temperature hydrothermal fluids are discharged into the ocean, often as "black smokers" characterized by steep gradients of temperatures between 400°C and 2°C over centimeter spatial scales. Abundant minerals grow in such temperature gradients leading to the formation of hydrothermal chimneys. The sequence of nucleation and growth of the main mineral phases (e.g. pyrite, sphalerite, chalcopyrite,...) is relatively well known. I will first discuss the mineral assemblages observed in these systems using a geochemical code (Chess). Predictions regarding nucleation and growth of accessory minerals, some of them having not been described in these environments yet, will then be made using the same geochemical code. This modeling will be used in further studies as a guide for searching such phases in natural samples collected from oceanographic campaigns lead by IFREMER, Brest, France.

Hyperthermophilic microorganisms (i.e. optimally living above 80°C), mostly archaea, inhabit hydrothermal chimneys, although their direct imaging within the porosity of the rocks has not been accomplished yet. Organic matter is observed in close association with minerals, in particular pyrite, but it is not clear whether that organic matter is related to hyperthermophilic microorganisms or to abiotic organic synthesis which is known to occur in these natural environments. The main questions we will discuss in this lecture are thus related to the nucleation and growth of minerals induced by such microorganisms living under the most extreme conditions (for life) as listed below :

- (1) Are biom mineralization processes at work in these hydrothermal chimneys?
- (2) Can mineral traces of hyperthermophilic microorganisms be recognized in these environments?
- (3) What is the interplay between biological and abiotic synthesis of reduced carbon compounds in these systems and which role minerals might play in those processes?

Among archaea inhabiting hydrothermal chimneys, the genus *Thermococcus* been shown to be dominant at several locations. In recent experiments specifically designed to study the biom mineralization by hyperthermophilic microorganisms, we have shown that nucleation and growth of pyrite and of greigite occur at 85°C in close association with cells of several species of the genus *Thermococcus*. FeS_2 pyrites were formed by reaction of sulfur-rich vesicles with Fe^{2+} and since most vesicles were still attached to the cells, there was a remarkable co-localization of pyrite minerals with the cells. Fe_3S_4 greigite precipitated on extracellular polymeric substances (EPS) in the immediate vicinity of cells and we could show that the adsorption of Fe^{3+} on the EPS prevented pyrite precipitation and favored the formation of greigite. This result is particularly significant because greigite has a strong catalytical potential toward CO_2 reduction thus promoting abiotic organic synthesis. Such situations in which biom minerals promote abiotic

organic synthesis illustrate the complexity of the abiotic/biotic conundrum of the organic matter production in hydrothermal systems. Thermodynamic models using Chess show that the nucleation of greigite is not favored in any possible precipitation sequence and that the presence of iron (III) phosphate on EPS might be the only way to prevent the thermodynamically stable pyrite formation. In that sense, greigite in the environment of hydrothermal chimneys could constitute a biosignature but this difficult notion will be then discussed.

In addition to the metabolism of S(0) reduction described above, both metabolisms of Fe(II) oxidation and Fe(III) reduction are favourable to biomineralization. Iron (III) reducing bacteria and archaea are particularly interesting because they commonly produce magnetites. Magnetites are extremely valuable environmental markers amenable to concentration by magnetic separation techniques permitting the accumulation of sufficient material for detailed geochemical studies often lacking due to low abundances of biominerals. We recently have demonstrated the quality of the magnetite geochemical biomarker in the specific case of (non hyperthermophilic) magnetotactic bacteria. Although not directly relevant to hydrothermal biomineralization, I will show how this example might contribute to the strategy of search for biomineral signatures in hydrothermal chimneys.

Finally, in a more prospective way, I will discuss three applications that might be generated by a better understanding of nucleation and growth of minerals induced and/or controlled by hyperthermophilic microorganisms.

- (1) Hyperthermophilic strains have the potential to immobilize metal elements in insoluble mineral phases. Having a bioremediation reactor based on biomineralization by hyperthermophilic microorganisms would enable all the advantages of bio processes (e.g. green chemistry, high

specificity) while taking advantage of better kinetics and avoidance of any contamination of the reactor with undesired microorganisms.

- (2) Interactions between minerals and microorganisms thriving at high temperature could be highly beneficial for bio-extraction of specific elements from minerals in bio-hydrometallurgical processes.
- (3) One particular area which has not been explored above 90°C yet is the bio-production of solid phases of interest for technological applications such as catalysis, electrochemistry (e.g. battery materials) thus filling a gap existing between low temperature bio-assisted synthesis of technological nanomaterials and higher temperature hydrothermal synthesis or processing. The bio-assisted synthesis of materials above 100°C could allow to combine the interests of two synthesis routes for now still antagonistic.

Crystallization in acidic media: from nanoparticles to macrocrystals

/ Javier Sanchez España

Instituto Geológico y Minero de España, Calera, 1, 28760, Tres Cantos, Madrid, Spain. j.sanchez@igme.es

Abstract

Crystallization in acidic media obeys the same rules and physico-chemical principles than in any other aqueous solution. However, the composition (mineralogy), particle size and crystallinity of the solids formed in these low pH systems are strongly determined by (i) the singular water chemistry of the parent acidic solutions (highly concentrated, with presence of many dissolved metals, and usually dominated by the sulfate anion, SO_4^{2-}), and (ii) the highly variable environmental conditions prevailing in the crystallization media (which may range from very fast to slow precipitation kinetics, from strong oversaturation to near solubility equilibrium, or from high to low density of nucleation centres). The most common mineral groups formed in acidic waters (e.g., acid mine waters, acid rock drainage) are usually metal sulfates, oxy-hydroxysulfates and sulfides, which expand largely in size (from nano-particles with diameters < 100 nm to large crystals of mm- to cm-scale) and crystalline order (nearly amorphous or short-range ordered to highly crystalline).

Key-words: sulfates, sulfides, nanoparticles, crystal growth, kinetics, mineral solubility, acidic waters

1. Introduction

Crystallization is commonly defined as the process (natural or artificial) by which a solid is formed after atom or molecule organization in a well-defined structure known as a crystal (Mullin, 2001). In the majority of cases, this process takes place in an aqueous solution through precipitation at low (ambient) temperature, though it may also take place from a melt or from a gas at higher temperatures. Crystallization and precipitation are therefore closely related concepts. The difference between them is that in the former case the product is always ordered (the crystal), while in the later, the solid may also be amorphous or disordered.

Crystallization in acidic media obeys exactly the same rules and identical physical and chemical principles than in any other aqueous solution. However, the particular nature and chemical features of *natural* acidic waters imposes certain restrictions and general trends which affect to a great extent the crystallinity (=degree of structural order within the crystal) and size of the formed solids in these solutions. Here, the term "*natural*" refers to the fact that acidic solutions form spontaneously as a result of natural chemical reactions (e.g., pyrite oxidation), even if such reactions occur in deeply anthropogenic and severely man-modified environments, such as mining operations or waste disposal sites.

In addition to the parameter which most obviously defines these waters (i.e., high acidity, low pH), the singular water chemistry of what is commonly referred to as *acid mine drainage* (AMD) or *acidic mine waters*, includes characteristics such as (i) very high solute concentrations and ionic strengths which largely exceed those usually encountered in dilute solutions and fresh waters, (ii) presence of many dissolved metals (e.g., Fe, Al, Cu, Zn, Mn) and metalloids (e.g., As), resulting from the dissolution of different reacti-

ve minerals, and (iii) omnipresence of the sulfate anion (SO_4^{2-}), as a natural consequence of sulphide (mostly pyrite) dissolution, and which determines the ionic complexes forming in the solutions (metal-sulfate complexes) and the mineralogical nature of the solids formed, dominated by sulfates, oxy-hydroxysulfates and/or secondary sulfides, depending on the pH and redox conditions (Nordstrom & Alpers, 1999a).

The environmental conditions prevailing in the crystallization media may also be highly variable (e.g., totally anaerobic and highly reducing to fully oxygenated and oxidising, running waters with turbulent flow to standing waters with laminar or negligible flow, abundance or scarcity of microorganisms, etc...), thus leading to notably different crystallization patterns and resulting mineral products. This variability affects to critical aspects such as (i) precipitation kinetics (from very fast to slow), (ii) saturation state (from strong oversaturation to near solubility equilibrium), or (iii) abundance or scarcity of nucleation centres (high to low density).

In this review, I firstly provide some brief fundamentals on crystallization and acid mine water chemistry, and then I describe the most important solids (nearly amorphous or short-ranged ordered to highly crystalline) forming in acidic waters, along with the chemical conditions leading to their formation (precipitation or crystallization), and the main mineralogical characteristics of these solids. For simplicity, these solids are grouped by mineral types and chemical environments.

2. General concepts of crystallization

The process of crystallization consists of two major stages, *nucleation and crystal growth*. These two stages are both controlled by well-known thermodynamic and kinetic principles. In nucleation, the solutes (atoms, molecules) originally dispersed in the solution start to group into clusters which increase the solute concentration in micro-scale regions. These regions

of higher solute density and cluster rearrangement are called the *nuclei*. Crystal growth is the stage by which nuclei that reach a *critical size* (which is controlled by temperature or supersaturation) become larger in size due to farther atom or molecule incorporation. The arrangement of atoms around the nuclei takes place in a periodic and well-defined manner, which defines the *crystal structure* (Ashcroft & Mermin, 1976).

Crystal growth is essentially a dynamic process and usually occurs under equilibrium conditions, where atoms or molecules precipitate out of solution or dissolve back into solution depending on the solubility (K_{sp}) of the species involved. Depending on the conditions in the crystallization medium, nucleation may predominate over crystal growth, or crystal growth may predominate over nucleation, and this balance dictates crystal size (more abundant crystals of smaller size in the former case, and fewer crystals of larger size in the latter). Nucleation and crystal growth are both under kinetic, more than thermodynamic, control.

2.1. Nucleation

Nucleation may be *homogeneous or heterogeneous* depending on whether it takes place directly from the solution without the participation of any solid surface or, on the other hand, it occurs with the mediation of solid surfaces which catalyse and make the process possible (e.g., Yang & Qiu, 1986). Purely homogeneous nucleation is a highly energy-demanding process (requires an important amount of activation energy), and rarely occurs in nature. Thus, nucleation is commonly heterogeneous and catalysed by any pre-existing solid surfaces, which may comprise from colloidal or dust particles to bacterial cells.

In another classification (somehow comparable to the former), nucleation is also commonly divided into *primary and secondary* nucleation, with the former comprising the early stages of nucleation taking place in the solution with no presence of crystals or solids, and the later involving the subsequent stages of crystal for-

mation with an important influence of the formed crystals, which would act as *seeds* favouring and catalysing the formation of more nuclei in the interface between the solution and the crystal surfaces.

The nucleation rate is usually defined by the following equation (Tavare, 1995):

$$B = [dN/dt] = k_n (c-c^*)^n \quad (1)$$

Where B is the number of nuclei formed per unit volume and unit time, N is the number of nuclei per unit volume, K_n is the rate constant, c is the solution concentration in a given time, c^* is the solution concentration at saturation, and n is an empirical exponent which usually ranges between 3 and 4. The term $(c-c^*)$ is usually known as the supersaturation value, and basically defines the quantity of solute available for the growth of the crystal.

2.2. Saturation and precipitation kinetics

Supersaturation is a major driving force of crystallization in aqueous media. The degree of saturation of a given solution with respect to the solubility of a certain solid is usually defined as the saturation index, SI, by the expression:

$$SI = \text{Log} [IAP/K_{sp}] \quad (2)$$

Where, IAP is the ionic activity product, and K_{sp} is the solubility product constant of the solid. Under equilibrium conditions, SI approaches zero ($SI=0$). When the concentration of solutes forming a given mineral phase is well below a critical value (the solubility product constant, K_{sp}), SI is negative and indicates that no nucleation or crystallization of that mineral will take place. On the other hand, when the solute concentration reaches the critical solubility limit, then SI becomes positive and the mineral may start precipitating out of solution. The higher the SI value, the more supersaturated is the solution, and the more thermodynamically favourable is the precipitation of that mineral.

Although there is not a direct relation between SI and the kinetics of the precipitation

process, as discussed below, the near-zero SI values indicating solubility equilibrium are usually associated with slow precipitation and crystallization kinetics (also with low nucleation rates, B), where the physical conditions (i.e., crystallization predominating over nucleation) favour the formation of fewer but larger and highly-ordered, crystalline solids. On the other hand, when a high chemical (e.g., pH, redox) disequilibrium occurs in the solution, the saturation indices may become abruptly very high as a natural response to quickly changing physico-chemical conditions. Under these circumstances, B (in equation 1) may be higher, nucleation and precipitation kinetics faster, nucleation predominates over crystallization (more abundant nuclei) and the resulting solids usually show lower crystal size (diameter) and crystalline order. Examples of the first situation related to acidic mine waters include evaporative pools with concentrated brines or porewaters within sediments, with no or negligible motion, and in which solute concentration eventually reaches the solubility limit, so that macroscopic crystals start forming and develop in the bulk solution or in interstitial space between soil or sediment particles. Examples for the second situation include anoxic waters emerging from mine portals or seeping from tailings or waste piles, and which suddenly get in contact with atmospheric O_2 which oxidizes reduced substances and provoke the appearance of oxidized species with much lower solubility compared to their reduced counterparts (e.g., Fe^{3+} as compared to Fe^{2+}), or mixing zones between acidic effluents and pristine water courses which provoke sharp pH gradients in spatially very restricted areas (e.g., often in a cm- or mm-scale). These environments are usually associated with low particle sizes and low degrees of crystalline order.

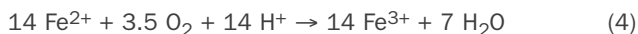
3. Chemistry of typical acid mine drainage solutions

Apart from being one of the most important (and most extensively studied) chemical reactions occurring in nature, the oxidation of pyrite is also responsible for the

formation of acidic mine drainage (Singer & Stumm, 1970; Nordstrom & Alpers, 1999a). The oxidation of pyrite in the presence of oxygen and water is chemically described by the reaction:



A very important chemical reaction associated with pyrite oxidation is the subsequent oxidation of the ferrous iron released in reaction (3), which is defined by reaction (4):



In the absence of molecular oxygen, ferric iron (Fe^{3+}) can also oxidize pyrite through reaction (5):



This second oxidation pathway is, in fact, much faster than the oxygen pathway (Garrels & Thompson, 1960; McKibben & Barnes, 1986).

Under acidic conditions (e.g., $\text{pH} < 3.5$), reaction (4) is much slower than reaction (3), so that the oxidation of Fe^{2+} by oxygen is considered the *rate-limiting step* (Singer & Stumm, 1970). The presence of acidophilic bacteria, however, accelerates the oxidation rate by a factor of $\sim 10^6$ with respect with the abiotic rate (Singer & Stumm, 1970; Nordstrom & Alpers, 1999a). Thus, microorganisms play a critical role in pyrite oxidation and AMD generation by maintaining a high concentration of ferric iron in the system. Oxygen will always be required to replenish the supply of ferric iron according to reaction (4), so that the overall rate of pyrite oxidation in a tailings or waste pile or in an underground mine will largely depend on the overall rate of oxygen transport by advection and diffusion (Nordstrom & Alpers, 1999a; Ritchie, 2003).

The stoichiometry of reaction (3) shows that the oxidation of pyrite inevitably leads to acidic solutions with dissolved iron and sulfate as major solutes. The concentration of acidity (protons, H^+), iron and sulfate in the solutions, as well as the redox state of iron (ferrous vs. ferric) will depend on many different factors, including: (i) residence time of the water body (e.g., aquifer) or stream (e.g., effluent) within the mine or waste (=reaction time), (ii) [rock/water] ratio, (iii) pyrite content within the rock matrix, (iv) grain size (the smaller the more reactive), (v) concentration and metabolic activity of acidophilic, iron-oxidising bacteria in the mine sites, or (vi) temperature (which affects the bacterial metabolism to a great extent), to name only a few. Many acidic mine waters around the world may exhibit sulfate and iron concentrations in the order of hundreds of mg/L and up to tens or even hundreds of grams per liter (g/L) in the most extreme cases (e.g., Nordstrom & Alpers, 1999b; Alpers et al., 2003; Sánchez-España et al., 2008). In addition, the low pH of these acidic waters provokes the dissolution of reactive minerals present in the host rocks, such as other sulfides (e.g., sphalerite, chalcopyrite, arsenopyrite, galena), carbonates (e.g., calcite, siderite) or aluminosilicates (e.g., feldspar, chlorite, illite/muscovite). Therefore, AMD waters usually include very high concentrations of many others metals (e.g., Al, Mn, Cu, Zn, Co, Ni, Cd) and metalloids (e.g., As), in addition to other alkaline and alkaline earth metal cations (e.g., Mg, Ca, Na, K).

The redox chemistry of AMD is mostly controlled by the iron redox chemistry, which is in turn controlled by the availability of O_2 , as discussed before (reaction 4). In deep underground mines or within tailings and waste piles, the rate of oxygen consumption largely exceeds the replenishment of O_2 through advection and diffusion, and waters are usually anoxic (i.e., devoid of oxygen), so that ferrous iron stays reduced in a large proportion. On the other hand,

at near-surface conditions, O₂ is more readily available (it is not a limiting reactant), and iron is oxidized at rates commonly typical of bacterial mediation (Nordstrom, 1985; Sánchez-España et al., 2007a).

4. Oxy-hydroxysulfate nanoparticles resulting from Fe(III) and Al precipitation

The conventional assumption defines nanoparticles as those having sizes comprised between 1 and 100 nm (e.g., Hochella, 2008). The biogeochemical conditions of acid mine waters favor the precipitation of certain mineral phases which tend to form particles with sizes close to this limit of particle size, and therefore can be considered as nanoparticles. These nm-sized particles may later coalesce and form mineral aggregates of larger (e.g., sub-micron) size, but when observed under SEM or TEM, it is often possible to identify the original nanometric units forming those aggregates. Their small size makes them behave as colloids in the solutions (i.e., they do not settle and their physical transport may be comparable to that of solutes). This small size also confers these particles a very high specific surface area and a very high sorbent capacity, which make these phases an important element in the transport of many contaminants (heavy metals and metalloids) and critical nutrients (e.g., phosphate, organic compounds). The two most classical and important examples are those of schwertmannite (an Fe(III)-oxyhydroxysulfate resulting from ferric iron precipitation at pH 2.5-4.0) and hydrobasaluminite (an Al-bearing oxyhydroxysulfate formed by Al³⁺ precipitation at pH>4.0). These two minerals have very low crystallinity, though they are not amorphous at all. Instead of well-defined, narrow peaks, their XRD patterns show broad reflections diagnostic of short-range order (Bigham et al., 1996; Bigham & Nordstrom, 2000; Sánchez-España, 2007; Sánchez-España et al., 2011).

4.1. Schwertmannite and its transformation to jarosite crystals

The solid formed by precipitation of Fe(III) in AMD solutions at pH 2.5-3.5 is usually schwertmannite (Bigham et al., 1994, 1996; Bigham & Nordstrom, 2000, Kawano & Tomita, 2001). The precipitation of schwertmannite is given by the reaction:



The crystal system of this mineral is tetragonal-dipyramidal (P 4/m), with an akaganéite-like structure, Fe³⁺ atoms in octahedral coordination and bridging complexes between Fe and SO₄ (Singer & Stumm, 1970). Under experimental conditions (e.g., during titration with fast precipitation rate) it may form pseudo-spherical particles with diameters around 100 nm (Fig. 1a), though its more typical morphology is usually that of hedgehog (or pin-cushion), which is composed of nanometric needles or whiskers with thickness <4-5 nm and lengths of 50-100 nm (Fig. 1b-d) (Bigham et al., 1994, 1996; Sánchez-España et al., 2011, 2012, 2016a).

The occurrence of schwertmannite is closely associated with the presence of iron-oxidising, acidophilic bacteria, which are needed to oxidize Fe(II) to Fe(III) at low pH, as discussed previously. For this reason, the acicular, needle-like morphology of this mineral has been sometimes interpreted to result from biomineralization or mineral encrustation of rod-like bacterial cells (e.g., Ferris et al., 2004). However, different laboratory studies have shown that the presence of bacteria is not actually needed, and hedgehog schwertmannite may also form under purely abiotic conditions (e.g., Goetz et al., 2010). The needles forming the structure of schwertmannite particles are more likely the result of preferential mineral growth along a specific direction, and seems to be kinetically (not biotically) controlled.

An important aspect about the geochemistry of schwertmannite is that, although its formation is kinetically favored with respect to other iron-bearing phases and this mineral is usually

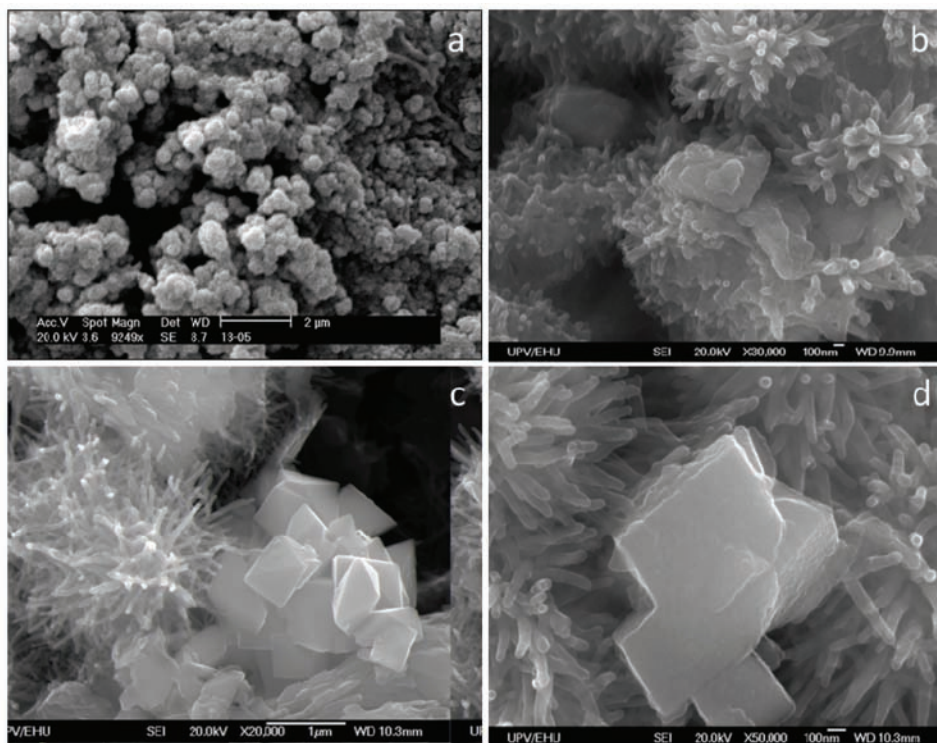
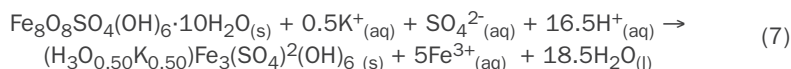


Fig. 1. Schwertmannite particles formed by ferric iron precipitation in acidic waters at pH 2.5-3.5: (a) globular schwertmannite particles formed in the lab during titration of acidic solutions with NaOH 1 M; (b-d) natural schwertmannite particles found in the acidic pit lake of San Telmo (Huelva, Spain) showing characteristic hedgehog morphology, and coexisting with euhedral crystals of jarosite. Compiled from Sánchez-España et al., 2011, 2012, with permission.

the first product of Fe(III) precipitation in the pH window of 2.5-4.0, it is metastable and tends to transform to other mineral phases such as jarosite or goethite, depending on the hydrochemical conditions (pH, pe, SO_4 concentration, etc.) (Bigham et al., 1996; Bigham & Nordstrom, 2000; Sánchez-España et al., 2011). Under low pH (e.g., <2.5-3.0) and high sulfate concentrations ($\sim 0.1 \text{ M SO}_4^{2-}$), jarosite is usually the more stable ferric iron mineral. The mineral transformation of schwertmannite to jarosite may take place in the sediments of acidic streams and lakes (e.g., Regenspurg et al., 2004; Acero et al., 2006; Jönsson et al., 2005) or directly in the water column of lakes or acidic reservoirs (e.g.; Sánchez-España et al., 2011, 2012) (Fig. 1c-d). Thus, it is rather common to observe hedgehog schwertmannite coexisting with euhedral crystals of jarosite which have been formed by transformation of the former (Fig. 1c-d). Jarosite formed in these acidic environments can be variable in composition (e.g., from potassium jarosite to hydronian jarosite), though the most common case is that of a solid solution with variable amounts of K+ and H_3O^+ in the alkali site (Alpers et al., 1989; Dutrizac & Jambor, 2000; Stoffregen et al., 2000; Sánchez-España et al., 2012). Thus, the conversion of schwertmannite to jarosite can be represented by the reaction:



This transformation may comprise different stages of dissolution and reprecipitation in a manner that it is often possible to observe newly formed jarosite crystals with remnant schwertmannite whiskers which still have not been replaced (Fig. 2).

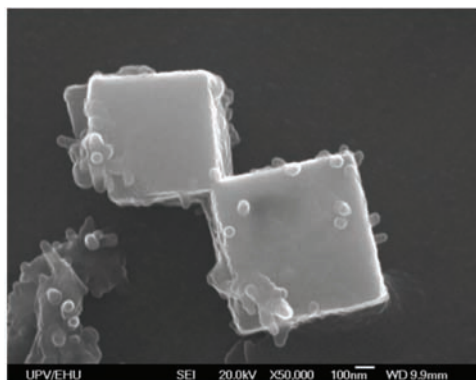
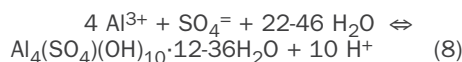


Fig. 2. Pseudocubic crystals of jarosite formed in San Telmo acidic pit lake (Huelva, Spain) after transformation of former schwertmannite needles, some of which can still be observed. Reprinted from Sánchez-España et al., (2012) with permission from The Mineralogical Society of Great Britain and Northern Ireland.

4.2. Hydrobasaluminite and its transformation to Al oxides and/or aluminosilicates

Another process which also leads to sub-micron- to nanoparticle formation in acidic systems is the precipitation of aluminum. In fresh dilute waters this process usually takes place at pH around 5.0, when Al flocs (typically consisting in gibbsite or amorphous $\text{Al}(\text{OH})_3$) precipitate out of solution (Nordstrom & Ball, 1986; Furrer et al., 2002). In solutions with high sulfate concentration (e.g., AMD), however, this process takes place at comparatively lower pH (around 4.0-4.5) and the solid formed is usually a nearly amorphous oxyhydroxysulfate with stoichiometry between hydrobasaluminite and felsöbanyaite

(Nodstrom, 1982; Bigham & Nordstrom, 2000; Sánchez-España, 2007; Sánchez-España et al., 2006, 2011, 2016b). The hydrolysis of Al^{3+} to form hydrobasaluminite is described as follows:



The size and morphology of the hydrobasaluminite particles formed by reaction (8) largely depends on precipitation kinetics, which may in turn vary from fast precipitation rates in mixing zones with very sharp pH gradients leading to oversaturation, to slow rates in near-equilibrium or slightly saturated systems (e.g., water column of acidic lakes). Under SEM, most particles are pseudo-spherical and around 1 μm in diameter (Fig. 3a), and the XRD analyses can only detect two broad reflections near 7° and $20^\circ 2\theta$ (Fig. 3b).

However, detailed investigations by TEM have revealed that the diameter of some hydrobasaluminite particles can be much smaller (as low as 100-200 nm) and may even show certain crystal faces indicative of partial recrystallization (Fig. 4a). Further, hydrobasaluminite is known to be metastable with respect to other Al phases, such as oxides (e.g., gibbsite, bayerite) or aluminosilicates (e.g., allophane), so that nanometer-scale crystals of the latter minerals can be observed in the sponge-like amorphous matrix of the

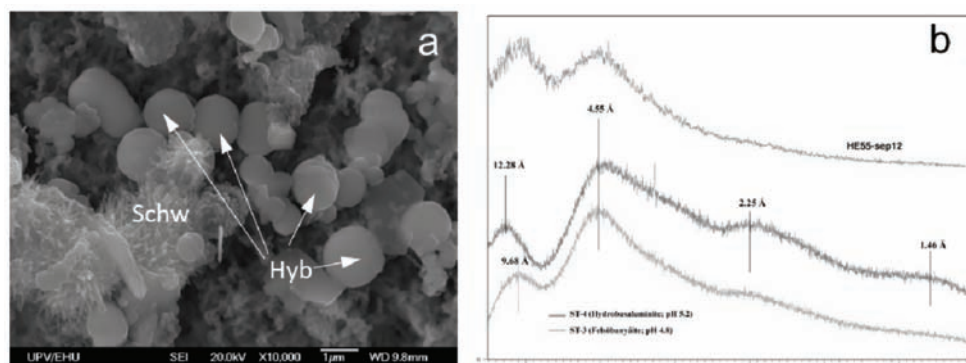


Fig. 3. a) SEM picture of hydrobasaluminite (Hyb) particles found at depth in the Guadiana acidic pit lake (Huelva, Spain); schwertmannite (Schw) particles with hedgehog morphology are also observed coexisting with the hydrobasaluminite. (b) typical XRD patterns of hydrobasaluminites formed by titration in the laboratory (ST-3 and ST-4) and naturally formed in the acidic pit lake of Guadiana (HER55). Reprinted from Sánchez-España et al., 2011 and Sánchez-España et al., 2016b, with permission.

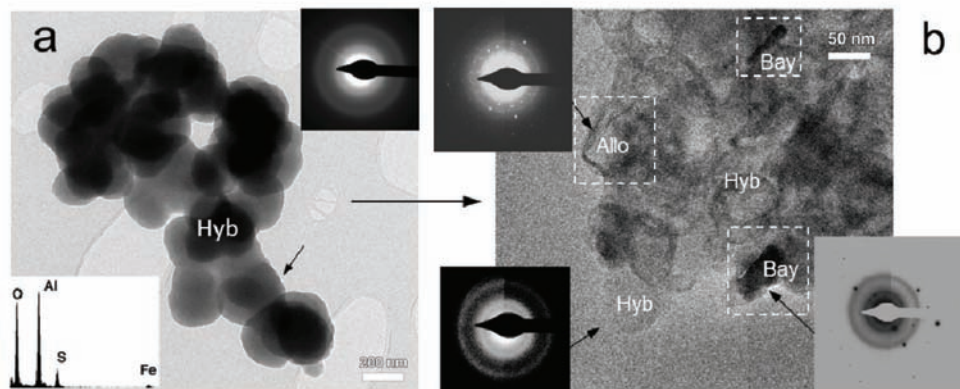


Fig. 4. aTEM images and associated EDS and SAED patterns of aluminum particles found in deep anoxic waters of the Guadiana acidic pit lake: (a) hydrobasaluminite (Hyb) cluster made of nanometric particles which range from subrounded to slightly faceted; (b) nanometric crystals of bayerite (Bay) and allophane (Allo) embedded in amorphous hydrobasaluminite matrix (Hyb). Reprinted from Sánchez-España et al., (2016b), with permission.

hydrobasaluminite globules, which has been interpreted as diagnostic of recrystallization and mineral replacement (Fig. 4b; Sánchez-España et al., 2016b).

5. Direct crystallization of Fe-Al sulfates

In the previous section, the formation of crystalline (well-ordered) minerals was indirect and resulting from recrystallization of less stable precursor phases (i.e., jarosite from schwertmannite, bayerite from hydrobasaluminite; Figs. 2 and 4b). However, crystals of jarosite and its related Al counterpart (alunite) can also form directly from solution under certain geochemical and physical (hydrological) conditions (Sánchez-España et al., 2016a). Furthermore, because the molar concentrations of Fe(III) and Al in the acidic solutions is often comparable, and as far as the pH range of these waters falls within the stability field for both sulfate minerals, these two pure end-members are rarely seen in nature, and the most common case is to find intermediate members of the jarosite-alunite solid solution (Alpers et al., 1989; Dutrizac & Jambor, 2000; Sánchez-España et al., 2016a).

The geochemistry of certain acidic pit lakes favors the precipitation of well-developed crystals of jarosite and alunite, and the low turbulent hydrological conditions of these water bodies allow nucleation and

further crystalline growth. The combination of conventional SEM and TEM with high resolution TEM (HRTEM), cryo-TEM, and scanning transmission electron microscopy (STEM) has provided definitive evidence for the simultaneous formation of these two phases (Fig. 5c). Moreover, slight fluctuations of the pH conditions in the parent fluid during crystal growth may lead to zoned crystals which record these chemical variations and which can be used to deduce the recent geochemical evolution of these waters (Figs. 5-6).

These zoned crystal growths reflect different stages in the crystal formation in which Al atoms or Fe atoms are preferentially incorporated into the crystal lattice as a response to subtle chemical variations. The examples shown in Figs. 5c and 6 were interpreted to result from a nucleation and early alunite crystal growth phase at pH~3.3, followed by later jarosite crystallization at pH 2.2-2.3 (Sánchez-España et al., 2016a). Such difference of around 1 pH unit is important enough to preclude the hydrolysis of Al^{3+} atoms (pK1 $\text{Al}^{3+}\sim 5.0$) and thus their incorporation into the sulfate crystal, while the lower pH value still allows a significant hydrolysis and precipitation of Fe^{3+} (pK1 $\text{Fe}^{3+}\sim 2.2$). Such chemical fluctuations are typical in acidic mine waters as a response to seasonal climatic changes, so that these zoned sulfate crystals may be more common than it has been previously considered.

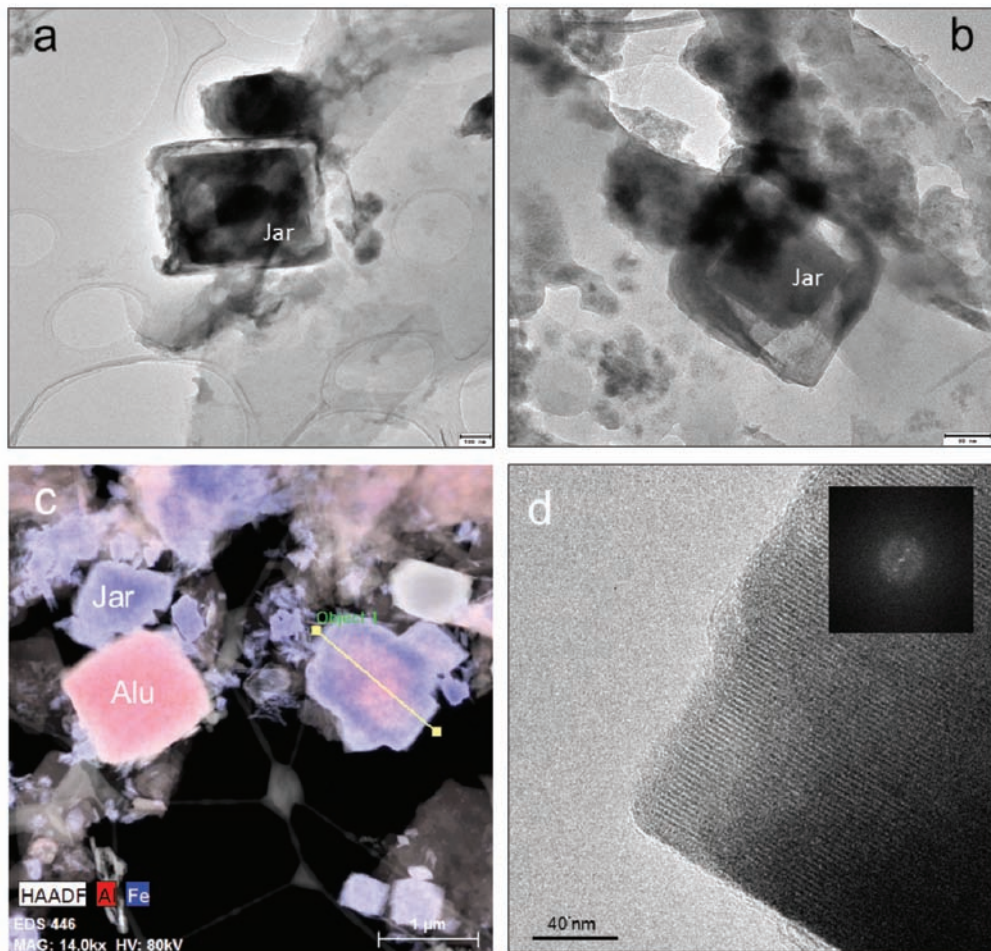


Fig. 5. TEM images of jarosite (Jar) and alunite (Alu) crystals found in San Telmo acidic pit lake: (a-b) zoned crystals of jarosite (scale bar is 100 and 80 nm, respectively); (c) STEM image and elemental mapping of jarosite and alunite end-members coexisting with a zoned crystal having an alunite core surrounded by a jarosite rim (Al shown in red, ferric iron shown in blue); (d) detail of crystalline planes in alunite crystal obtained by HRTEM. Modified from Sánchez-España et al., (2016a), with permission.

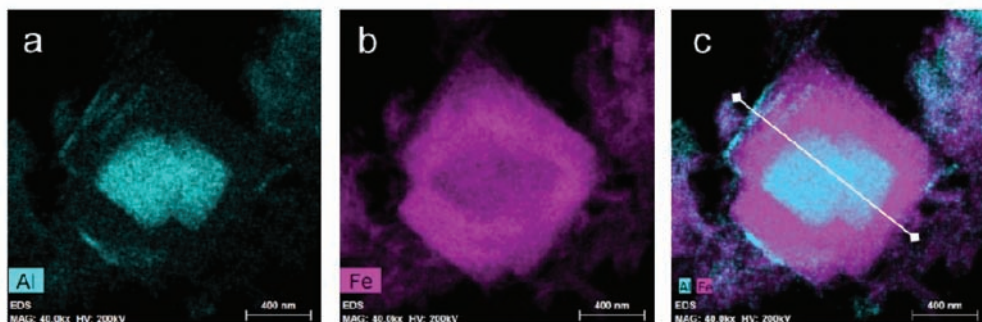


Fig. 6. STEM element mapping showing the Al (blue) and iron (pink) distribution in a zoned crystal precipitated in the water column of San Telmo pit lake (pH 2.2-3.3). Modified from Sánchez-España et al., (2016a), with permission.

Sometimes the crystallization process results in hopper crystals with fully developed edges and empty interiors (Fig. 7). This particular crystal formation usually takes place when the crystal grows so rapidly that there

is not sufficient time (or material) to fill in the gaps. Under such conditions, electrical attraction is higher along the edges of the crystal, and this causes faster growth at the edges than near the face centers.

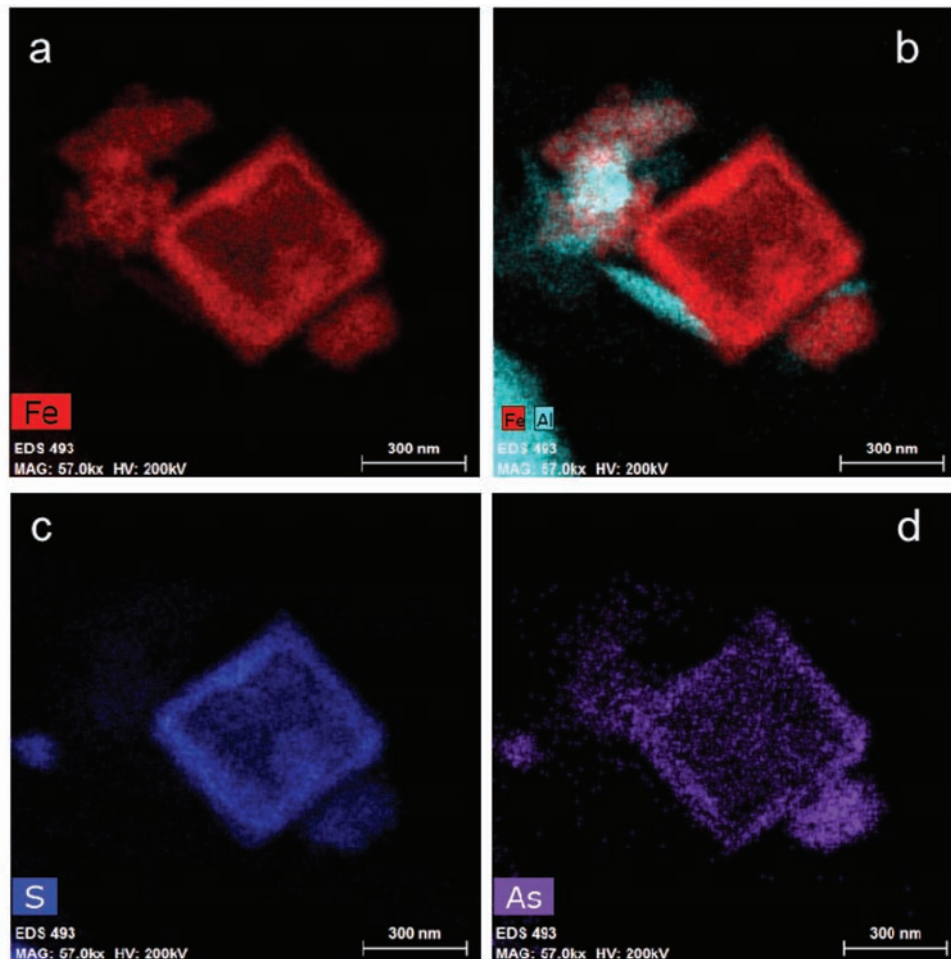


Fig. 7. STEM element mapping showing the distribution of Fe, S and As in a hopper crystal of jarosite formed in San Telmo pit lake. Reprinted from Sánchez-España et al., (2016a), with permission.

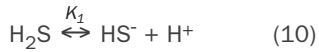
6. Metal sulfides formed in reducing and anoxic environments

Bacterial sulfate reduction can also take place at low pH (Koschorreck, 2008). The presence of sulfate-reducing bacteria (SRB, acidophilic or acid-tolerant) in sub-surface environments of acidic waters, under anoxic and highly reducing conditions, can lead to the production of hydrogen sulfide (H_2S) through the reaction:



where CH_2O represents organic matter .

This biogenic H_2S may then react with metals (e.g., Cu, Cd, Pb, Zn, Fe) or metalloids (e.g., As) to form different sulfide minerals, according to reactions (10-11):



where Me^{2+} represents a divalent metal cation such as Cu^{2+} , Zn^{2+} , Pb^{2+} , Cd^{2+} or Fe^{2+} (Lewis, 2010).

In a system where different dissolved metals are present, as is the case of most AMD environments, different sulfide minerals may precipitate according to their respective solubilities. Sulfide minerals increase in solubility

from CuS (covellite-like, the less soluble) to FeS (mackinawite-like, the most soluble), and as pH increases, a natural sequence of sulfide precipitation in different stages can be observed with the order usually being: $\text{CuS} > \text{CdS} > \text{PbS} > \text{As}_2\text{S}_3 > \text{NiS} > \text{ZnS} > \text{FeS}$ (Diez-Ercilla et al., 2014).

In a narrow layer situated immediately below the redoxcline at 11 m depth into the water column of the acidic pit lake of Cueva de la Mora (Huelva, Spain), Diez-Ercilla et al., (2014) found different metal sulfides resulting from the sequence of reactions (9-11). The presence and metabolic activity of SRB in this layer (Wendt-Phottoff et al., 2012; Falagán et al., 2014) produces H_2S which immediately reacts with dissolved Cu, As or Zn and precipitate at pH between 3.0 and 4.0. Careful examination by electron micros-

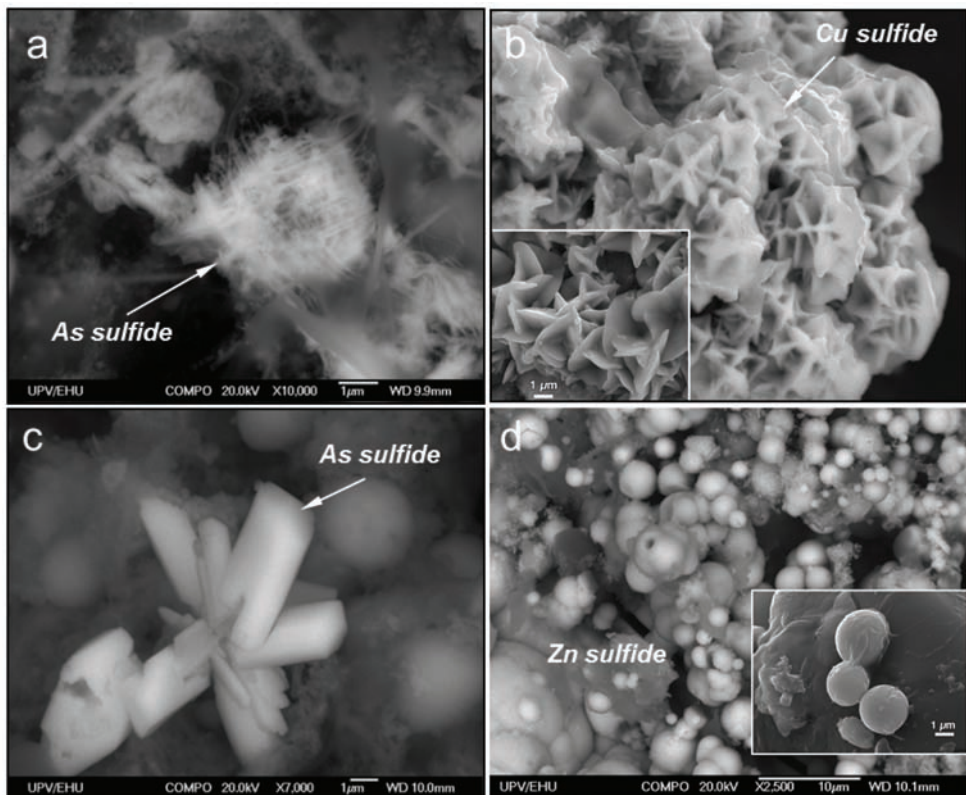


Fig. 8. SEM images of different sulfide minerals found at depth between 11 and 18 m in Cueva de la Mora acidic pit lake: (a) Aggregate with acicular crystals of As sulfide; (b) rosette-like platy crystals of natural Cu sulfide (covellite) – the inset shows a morphologically similar covellite growth obtained in the laboratory; (c) euhedral (prismatic) crystals of As sulfide; (d) spherical particles of amorphous Zn sulfide (likely wurtzite); the inset shows a detail of wurtzite particles analysed by EDS. Modified from Diez-Ercilla et al., (2014).

copy has revealed that these sulfides exhibit highly contrasting crystallinity and morphology, and it is common to observe nearly amorphous, pseudo-spherical particles (e.g., ZnS) coexisting with well-defined crystals (e.g., CuS, covellite; As_2S_3 , orpiment) (Fig. 8). Depending on the mineral, crystal habits may comprise whiskers, laths, rods, and also amorphous gel-like aggregates.

Arsenic sulfides show different morphologies, including web- and wire-like aggregates (Fig. 8a), fine granular, and well-formed, prismatic crystals in micrometric clusters (Fig. 8c). The S/As molar ratios, frequently close to S/As=1.3, are usually diagnostic of orpiment stoichiometry (As_2S_3). Amorphous As_2S_3 and orpiment are known to precipitate mainly at low pH and low sulfide concentration.

In contrast to the arsenic sulfides, zinc sulfides have been only identified as spherical ZnS particles (Fig. 8d). This spherulitic mor-

phology is common in fine-grained sphalerite (Labrenz *et al.*, 2000) and has been also found in sulfidic acid environments (e.g., Church *et al.*, 2007).

Copper sulfide precipitates have been also obtained in the laboratory by addition of Cu^{2+} (as CuSO_4) to solutions containing H_2S (Diez-Ercilla *et al.*, 2014). These Cu sulfides showed tabular growth with rosette-like aggregates (Fig. 8b). This crystalline morphology has been also occasionally observed in natural samples (Fig. 8b-inset). The obtained S/Cu molar ratios of these crystals (≈ 1), and electron diffraction patterns obtained by TEM (Fig. 9c) indicate that covellite is the most common Cu sulfide. This mineral can directly precipitate out of solution or, alternatively, it may also form by aging of primitive copper sulfide precursor (Patrick *et al.*, 1997; Luther *et al.*, 2002). The textural and microstructural features of covellite crystals, often surrounded by exopolymeric substances (EPS) excreted by the bacteria, and also in

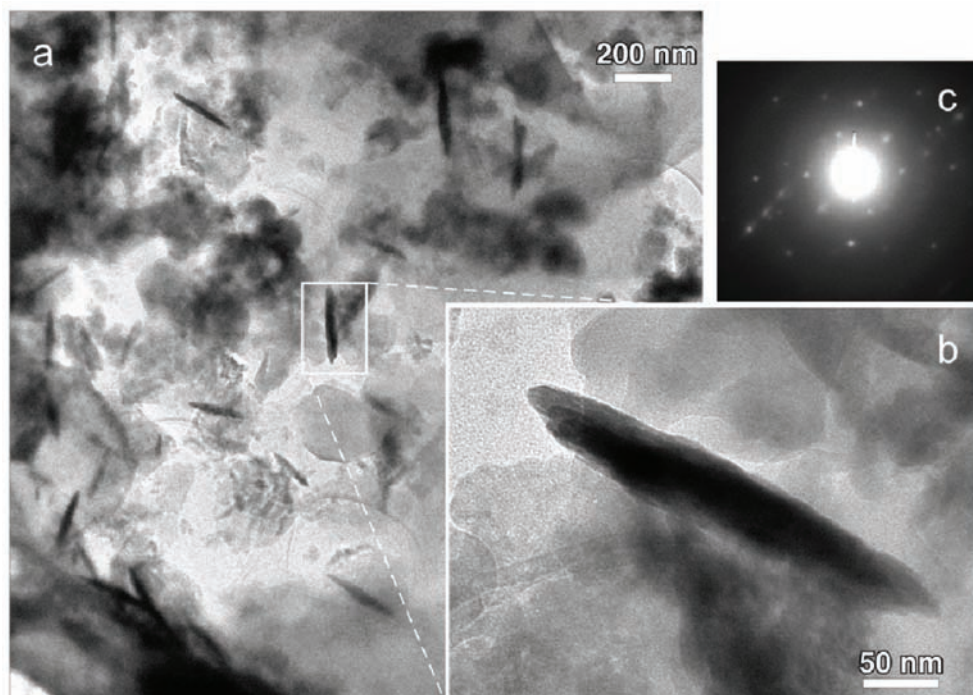


Fig. 9. (a) TEM picture of covellite crystals found at depths of 32 m in Cueva de la Mora acidic pit lake (pH 4.0-4.5); (b) Detail of (a) showing the elongated habit, nanometric width and sub-micron length of a covellite crystal embedded in amorphous matrix; (c) SAED pattern showing brilliant spots diagnostic of major crystalline planes of crystal in (b). Reprinted from Diez-Ercilla *et al.*, (2014), with permission.

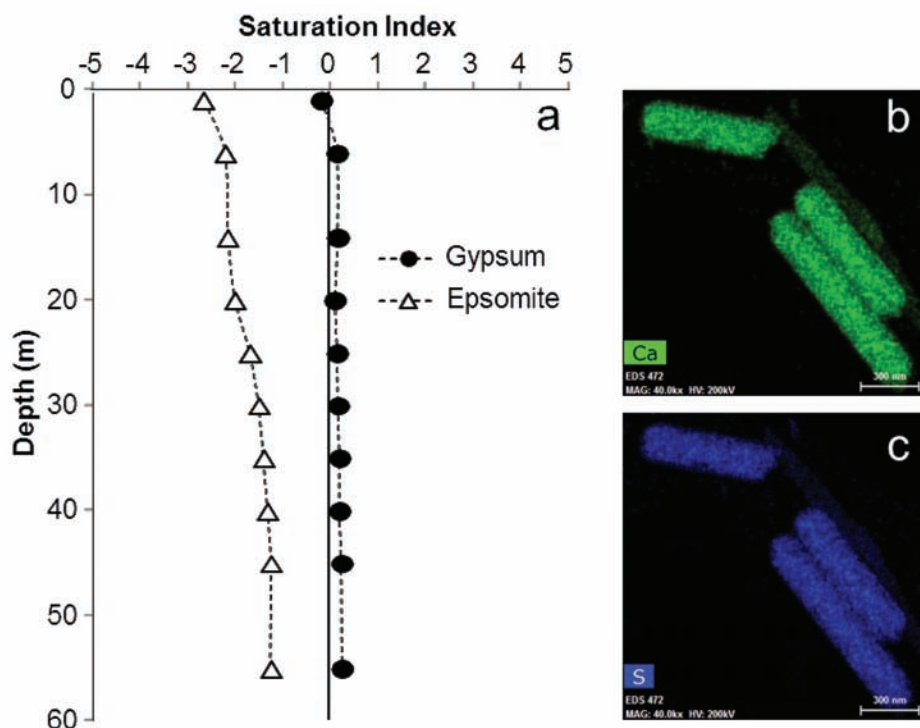


Fig. 10. (a) Vertical evolution of the saturation index (SI, defined as $SI = \log(IAP/K_{sp})$) of gypsum and epsomite, as a function of depth, in the Guadiana acidic pit lake (pH 3.0-4.2); (b-c) False-colour element mapping (obtained by STEM/EDS) showing Ca and S distribution in submicron-sized gypsum crystals naturally formed in the water column of this lake (30-40 m). Modified from Sánchez-España et al., (2014).

close association with amorphous gels of similar composition (CuS) (Fig. 9), suggest that the latter mechanism (i.e., indirect crystallization by crystalline re-arrangement of amorphous precursors) may be the most frequent pathway of covellite crystal formation in these acidic environments.

7. Precipitation of gypsum crystals

Another classical example of crystal formation in acidic solutions is that of gypsum ($\text{CaSO}_4 \cdot 2\text{H}_2\text{O}$). In acid-sulfate solutions, Mg is highly soluble and tends to be conservative (with the exception of evaporative pools), while Ca is less soluble and its aqueous concentration is normally controlled by gypsum solubility (Nordstrom, 2008). The precipitation of gypsum is thus the most important control of Ca concentration in acidic waters. This is often confirmed by geochemical calculations which show gypsum solubility equilibrium and under-saturation for Mg-sulfate

species (exemplified by epsomite). A good example of this is the acidic pit lake of Guadiana (Herrerías Mine, Huelva), where gypsum has been observed to form in the water column as a result of solubility saturation (Fig. 10). The plateau observed in Fig. 10a results from solubility equilibrium of Ca, and the maximum concentration of this element (up to 600 mg/L Ca) roughly equals the theoretical gypsum solubility limit at the sulfate concentrations found in the lake (5-25 g/L SO_4). Gypsum crystals have been frequently found in the water column of this lake, with idiomorphic (tabular) habit and sub-micron size (Fig. 10b-c).

Gypsum crystals can also form spontaneously in running acidic waters (e.g., mine effluents, AMD-impacted streams) and in treatment plants where base (often lime) addition to increase the pH of inflowing waters provokes gypsum solubility saturation. In these cases, gypsum is often found as well-

developed tabular crystals, although the length, diameter and habit of these crystals may differ depending on kinetic factors (chiefly, precipitation rate, which in turn depends on neutralization rate) (Fig. 11). Gypsum crystals found in different AMD environments can be as small as 500x100 nm (Fig. 10b-c) or as large as mm- to cm-scale (Fig. 11). Atomic substitution of Ca^{2+} for other divalent cations is not frequent, and gypsum crystals are often of high purity despite the metal-rich nature of the precipitating solutions.

If occurring during a sufficiently long time period, the precipitation of gypsum crystals in a given acidic system may remove a substantial amount of calcium from solution even at relatively low pH (e.g., 4.5-5.0), in contrast to other cations like Mg^{2+} , which require much higher pH values (usually above 9.0) to precipitate as an hydroxide or hydroxyl-carbonate (Sánchez-España & Yusta, 2015).

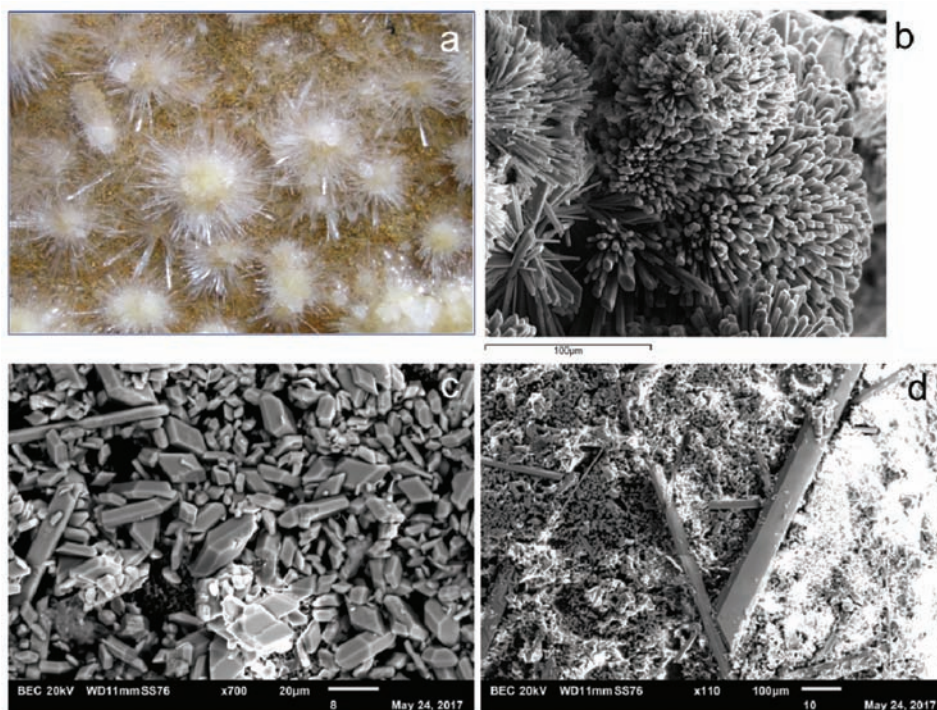


Fig. 11. Different examples of gypsum crystals formed in acidic mine waters: (a) Acicular gypsum crystals growing upwards from a streambed of an acidic mine effluent (field of view ~5 cm); (b) Rosette-like growth composed of columnar crystals of gypsum formed in the Tintillo acidic river; (c-d) prismatic crystals formed by neutralization of acidic solutions in the laboratory; smaller crystals of 10-20 mm length precipitated directly in the flasks, while the mm-scale crystals in (d) formed later during filtering and drying. (b) taken from Sánchez-España et al., (2007b).

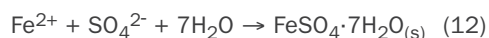
8. Formation of melanterite and rozenite crystals in evaporative, extremely acidic brines

The formation of efflorescent sulfates is typical in AMD waters and is especially abundant during spring and summer. The mineralogy of these soluble sulfates is closely associated with their spatial distribution and the pH of the brines from which these salts are precipitated (Nordstrom & Alpers, 1999b; Jambor et al., 2000; Nordstrom et al., 2000; Buckby et al., 2003; Sánchez-España et al., 2005; Velasco et al., 2005). Thus, Fe(II)-sulfates like melanterite, rozenite or szomolnokite are dominant in isolated and highly concentrated pools near the pyrite sources, under conditions typical of green, ferrous AMD with very low pH. On the other hand, mixed Fe(II)-Fe(III), and/or Fe(III)-Al sulfates like copiapite, coquimbite or halotrichite, are

common in the margins of rivers impacted by AMD, where iron has been partially oxidized and the pH is slightly higher (typically between 1.5 and 3). These sulfates have been observed to follow a paragenetic sequence with melanterite > rozenite > szomolnokite > copiapite > coquimbite > rhomboclase > halotrichite (Nordstrom & Alpers, 1999a,b; Jambor et al., 2000; Buckby et al., 2003; Velasco et al., 2005). Chemical analyses of mixtures of these sulfates have revealed very high metal contents (e.g., average values of 2,800 ppm Cu and 9,000 ppm Zn, with Zn values eventually reaching percent units; Sánchez-España et al., 2005), so that the precipitation-redissolution cycle of these salts is of high environmental relevance.

When acidic water stands in contact with pyrite during a sufficiently long period of time (long residence time and low water flow favouring mineral/water interaction), the combination of several chemical and physical processes can lead to the formation of extremely acidic waters with abnormally high concentrations of sulfate, ferrous iron and other metals (Nordstrom & Alpers, 1999b; Nordstrom et al., 2000; Alpers et al., 2003; Sánchez-España et al., 2008). The continuous dissolution of pyrite, coupled with the oxidation of Fe(II) to Fe(III) and the further oxidation of pyrite by Fe(III) within a relatively small water volume, provokes a continuous "iron wheel" which continuously solubilizes material and increases dramatically the solute concentration. If this process takes place in an arid or semi-arid region, where high ambient temperatures enhance pyrite dissolution and evaporation, the result may be an acid water with pH close to zero and sulfate concentrations in the order of hundreds of grams per litre. Under these conditions, the salinity and ionic strength is so high (e.g., several times that of seawater) that the conventional equations and activity coefficients used in common geochemical modelling software cannot be applied, since the electrostatic attraction and interaction between atoms in these brines is much more important than in dilute solutions, and deviations from the ideal behaviour can be very high (Nordstrom et al., 2000; Sánchez-España & Díez-Ercilla, 2008; Sánchez-España et al., 2008). In the most

extreme case known to date, Nordstrom et al., (2000) reported even negative pH values (due to H⁺ activity being higher than 1.0), sulfate concentration of 0.76 kg/L and dissolved iron concentration of 0.11 kg/L in waters found in Iron Mountain mine, California. In Spain, Sánchez-España et al., (2008) also reported the occurrence of green pools of extremely acidic water (pH 0.6) with similarly extreme concentrations of dissolved sulfate (134 g/L SO₄) and iron (61 g/L Fe_i) in San Telmo mine. Despite its low pH, however, this acidic liquor was close to saturation with respect to melanterite, and well-formed crystals were observed to precipitate directly from solution (Fig. 12a-b). The formation of these crystals occurs when the Fe²⁺ and SO₄²⁻ concentrations reach the solubility product constant for melanterite, and reaction (12) takes place until chemical equilibrium is attained:



The formation of crystals of melanterite and its associated mineral rozenite (FeSO₄·4H₂O) has been also observed in the margins of low-flow acidic streams with high Fe(II) concentrations (thus, close to the mining areas; Fig. 12c), and in porewaters in pyritic soils or sludges (Fig. 12d). The crystallization process in these environments usually takes place under hydrologically and kinetically favourable conditions (i.e., low flow or standing water, slow precipitation kinetics) which facilitate crystal growth. Thus, it is common to observe cm-scale macroscopic crystals showing well-developed concentric or parallel growths (Fig. 12b,d).

As discussed in a previous section, in addition of Fe²⁺, the acidic mine waters usually have very high concentrations of other divalent metal cations, such as Cu²⁺ or Zn²⁺. The size and atomic radius of these two cations is not very different from that of Fe²⁺, so that their incorporation into the melanterite crystal lattice is structurally possible, and Cu-rich and Zn-rich melanterites are frequent in these environments. As an example, some melanterite crystals shown in Fig. 12 displayed trace metal concentrations as high as 1.3 %wt. Zn and 0.7 %wt. Cu



Fig. 12. (a-b) Emerald-green melanterite crystals formed in extremely acidic (pH 0.6) ferrous sulfate brine solutions in contact with fine-grained pyritic sludge in San Telmo mine (Huelva). Photo (a) courtesy of Dr. Francisco Velasco (UPV/EHU), (a-b) from Sánchez-España et al., (2008); (c) Cu-rich, blue-coloured melanterite crystals forming an efflorescence in the margins of an evaporating acidic stream in San Telmo mine; (d) Large crystal of rozenite formed in pore waters of a soil with pyritic sludge in Tharsis mine (Huelva). The fields of view are 10 cm (a), 2 cm (b), 5 cm (c), and 8 cm (d).

(Sánchez-España et al., 2008; Sánchez-España & Diez-Ercilla, 2008).

The theoretical simulation of melanterite crystallization from these acidic brines through geochemical modelling must be accomplished by using models for concentrated solutions, as discussed before. The Pitzer specific-ion-interaction theory of activity correction for calculation of activity coefficients in brines and electrolyte solutions (Pitzer, 1986; Plummer et al., 1988) has been shown to work well in these aqueous systems. An example of melanterite precipitation model for the specific case of the San Telmo acidic brine was presented by Sánchez-España & Diez-Ercilla (2008) (Fig. 13). This model compared the solubility of melanterite (as defined by its saturation index) as calculated with the conventional Davis equation for

dilute solutions with that resulting of applying the Pitzer theory with Maclnnes convention. The plot shown in Fig. 13a shows that, as expected, the Davis equation cannot predict satisfactorily the precipitation of melanterite crystals at the chemical conditions prevailing in the parent solution, whereas the Pitzer/Maclnnes approach accurately establishes the beginning of melanterite crystallization at a sulfate concentration which roughly corresponds to that measured in the acidic liquor at the time of sampling. The application of the Pitzer approach also predicted cycles of melanterite crystallization followed by crystal re-dissolution as a response to natural diurnal temperature oscillations, with colder temperatures prevailing at night favouring crystallization, and hotter day-time temperatures favouring crystal re-dissolution (Fig. 13b).

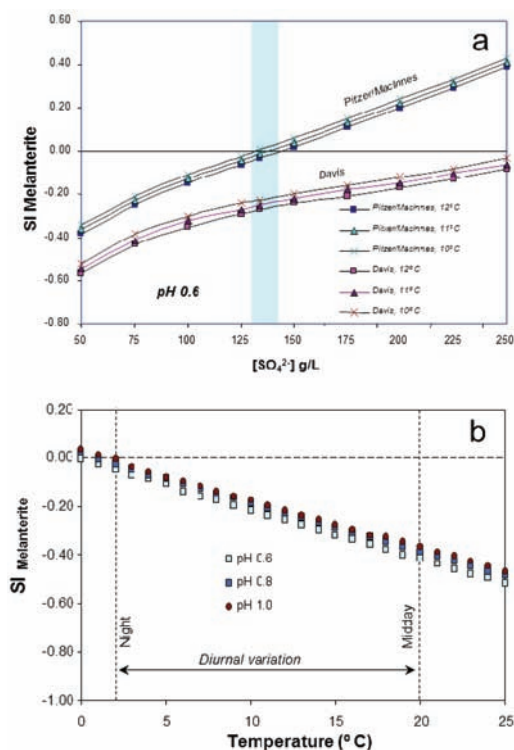


Fig. 13. Variation of the saturation index (SI) with respect to melanterite solubility as a function of sulfate concentration (a) and temperature (b) in an extremely acidic (pH 0.6) and ultra-concentrated liquor emanating from a pyrite pile in San Telmo mine (Huelva). In (a), the SI calculated for different temperatures and using two different approaches (Davis vs. Pitzer) are shown for comparison. The blue area indicates the range of sulfate concentration measured in this brine. In (b), the temperature-dependence of SI of melanterite is shown for different pH values and using the Pitzer/Maclnnes approach. The melanterite crystals formed in this environment are shown in Fig. 12(a-b). Modified from Sánchez-España et al., (2008) & Sánchez-España and Díez-Ercilla (2008).

9. Conclusions

The mineralogical composition, particle size and degree of crystallinity of the solids formed in low pH systems are strongly influenced by the chemical and physical factors which characterize this particular type of waters. Chemically, the singular chemistry of the parent acidic solutions usually includes highly concentrated, sulfate-rich waters with presence of many dissolved metals. Physically, the conditions prevailing in the crystallization media are highly variable and may range from very fast to slow precipitation kinetics, from strong oversaturation to near solubility equilibrium, or from high to low density of nucleation centres. In coherence with these chemical and physical conditions, the most

common mineral groups formed in acidic waters (e.g., acid mine waters, acid rock drainage) are usually metal sulfates, oxy-hydroxy-sulfates and sulfides, which expand largely in size and crystalline order. Particle or crystal sizes normally range from diameters < 100 nm (which are within the range of natural nano-particles and thus make them behave as colloids in the solutions) to large crystals of macroscopic (mm- to cm-) scale. The former sizes are usually associated with nearly amorphous or short-range ordered oxyhydroxysulfates (e.g., schwertmannite, hydrobasaluminite) formed in supersaturated solutions with relatively fast precipitation kinetics, but can also include nano- to sub-micron crystals precipitated directly from solution (e.g., gypsum) or by transformation of metastable precursors (e.g., bayerite or allophane from hydrobasaluminite recrystallization). The latter sizes are more often found in near-equilibrium environments where the slow crystallization kinetics allow formation of large and well-developed crystals. A classical example is the formation of melanterite or rozenite in super-concentrated acidic brines formed by evaporative processes near the oxidising-pyrite sources.

10. Acknowledgements

I would like to thank Dr Amalia Jimenez (Oviedo University, Department of Geology) and the Spanish Society of Mineralogy (SEM) for their kind invitation to present this talk at the “Crystallization under extreme conditions” workshop (Oviedo, July 4th, 2017). I also thank Dr Iñaki Yusta (Basque Country University, Department of Mineralogy) with whom I have shared so many hours of SEM and TEM work, as well as many vibrant discussions, during the last years. Pictures and information provided in this communication have been obtained during different research projects funded the Spanish Ministry of Economy (*Secretaría de Estado de Investigación, Desarrollo e Innovación*) through the *Plan Estatal de Investigación Científica y Técnica y de Innovación* (REN2003-09590-C-04-04, CGL2009-07090, CGL2016-74984-R), and the Spanish Ministry of Culture, Education and Sports (PRX14/00087).

References

- Acero, P., Ayora, C., Torrentó, C. & Nieto, J.M. (2006) The behaviour of trace elements during schwertmannite precipitation and subsequent transformation into goethite and jarosite. *Geochim. Cosmochim. Acta*, 70, 4130-4139.
- Alpers, C.N., Nordstrom, D.K. & Ball, J.W. (1989) Solubility of jarosite solid solutions precipitated from acid mine waters, iron Mountain, California, USA. *Sci. Géol. Bull.*, 42-4, 281-298.
- Alpers, C.N., Nordstrom, D.K. & Spitzley J. (2003) Extreme acid mine drainage from a pyritic massive sulphide deposit: The Iron Mountain end-member. (In J.L. Jambor, D.W. Blowes, & A.I.M. Ritchie (Eds.) *Environmental Aspects of Mine wastes, Mineralogical Association of Canada, Short Course Series Volume 31 (R Raeside, ed.)*, pp. 407-430, Vancouver, British Columbia.
- Ashcroft, N.W. & Mermin, N.D. (1976) Solid state physics. *Brooks/Cole*, 848 p.
- Battaglia-Brunet, F., Crouzet, C., Burnol, A., Coulon, S., Morin, D. & Jouliau, C. (2012) Precipitation of arsenic sulphide from acidic water in a fixed-film bioreactor. *Water Res.* 46, 3923-33.
- Bigham, J.M., Carlson, L. & Murad, E. (1994) Schwertmannite, a new iron oxyhydroxysulfate from Pyhäsalmi, Finland, and other localities. *Mineral. Mag.*, 58, 641-648.
- Bigham, J.M., Schwertmann, U., Traina, S.J., Winland, R.L. & Wolf, M. (1996) Schwertmannite and the chemical modeling of iron in acid sulfate waters. *Geochim. Cosmochim. Acta*, 60, 2111-2121.
- Bigham, J.M., Nordstrom, D.K. (2000) Iron and Aluminum Hydroxysulfates from Acid Sulfate Waters. In *Sulfate Minerals: Crystallography, Geochemistry, and Environmental Significance* (Alpers, C.N., Jambor, J.L., Nordstrom, D.K. (Eds.)). *Reviews in Mineralogy & Geochemistry*, 40, 351-403.
- Buckby, T., Black, S., Coleman, M.L. & Hodson, M.E. (2003) Fe-sulphate-rich evaporative mineral precipitates from the Río Tinto, southwest Spain. *Mineral. Mag.*, 67, 263-278.
- Church, C.D., Wilkin, R.T., Alpers, C.N., Rye, R.O. & McCleskey, R.B. (2007) Microbial sulfate reduction and metal attenuation in pH 4 acid mine water. *Geochem. Trans.* 8, 10-24.
- Diez-Ercilla, M., Sánchez-España, J., Yusta, I., Wendt-Phottoff, K. & Koschorreck, M. (2014) Formation of biogenic sulphides in the water column of an acidic pit lake: Biogeochemical controls and effects on trace metal dynamics. *Biogeochemistry* 121, 519-536.
- Dutrizac, J.E. & Jambor, J.L. (2000) Jarosites and their application in hydrometallurgy. In *Sulfate Minerals: Crystallography, Geochemistry, and Environmental Significance* (Alpers, C.N., Jambor, J.L., Nordstrom, D.K., Eds.). *Reviews in Miner. & Geochem.*, 40, 405-452.
- Falagán, C., Sánchez-España, J. & Johnson, B. (2014) New insights into the biogeochemistry of extremely acidic environments revealed by a combined cultivation-based and culture-independent study of two stratified pit lakes. *FEMS Microbiology Ecology* 87(1), 231-243.
- Ferris, F.G., Hallbeck, L., Kennedy, C.B. & Pedersen, K. (2004) Geochemistry of acidic Rio Tinto headwaters and role of bacteria in solid phase metal partitioning. *Chemical Geology*, 212, 291-300.
- Frau, F. (2000) The formation-dissolution-precipitation cycle of melanterite at the abandoned pyrite mine of Genna Luas in Sardinia, Italy: environmental implications. *Mineral Mag*, 64, 995-1006.
- Furrer, G., Phillips, B.L., Ulrich, K-U, Pöthig, R. & Casey, W. (2002) The origin of aluminum flocs in polluted streams. *Science* 297, 2245-2247.
- Garrels, R.M. & Thompson, M.E. (1960) Oxidation of pyrite by iron sulfate solutions. *Am J Sci*, 258A, 57-67.
- Goetz, A.J., Ziegler, A., Gaebel, J., Wiacek, C., Schlömann, M. & Schmahl, W.E. (2010) Structural variations in biogenic and synthetic schwertmannite. *Macla* 13, 118.
- Hochella M.F. (2008) Nanogeoscience: From origins to cutting-edge applications. *Elements* 4, 373-379.
- Jambor, J.L., Nordstrom, D.K. & Alpers, C.N. (2000) Metal-sulfate salts from sulfide mineral oxidation. In *Sulfate Minerals*. Alpers, C.N., Jambor, J.L. & Nordstrom, D.K (eds), *Reviews in Mineralogy and Geochemistry*, 40-6, 303-350.
- Jönsson, J., Persson, P., Sjöberg, S. & Lövgren, L. (2005) Schwertmannite precipitated from acid mine drainage: phase transformation, sulfate release and

- surface properties. *Appl. Geochem.*, 20, 179-191.
- Kawano, M. & Tomita, K. (2001) Geochemical modeling of bacterially induced mineralization of schwertmannite and jarosite in sulfuric acid spring water. *Am. Mineral.*, 86, 1156-1165.
- Kim, J.J. & Kim, S.J. (2003) Environmental, mineralogical, and genetic characterization of ochreous and white precipitates from acid mine drainages in Taebaeg, Korea. *Environ. Sci. Technol.*, 37, 2120-2126.
- Koschorreck, M. (2008) Microbial sulfate reduction at a low pH. *FEMS Microbiol. Ecol.* 64, 329–42.
- Labrenz, M., Druschel, G.K., Thomsen-Ebel, T., Gilbert, B., Welch, S.A., Kemner, K.M., Logan, G.A., Summons, R.E., De Stasio, G., Bond, P.L., Lai, B., Kelly, S.D. & Banfield, J.F. (2000) Formation of sphalerite (ZnS) deposits in natural biofilms of sulfate-reducing Bacteria. *Science* 290, 1744–1747.
- Lewis, A.E. (2010) Review of metal sulfide precipitation. *Hydrometallurgy* 104, 222–234.
- Luther, G.W., Theberge, S.M., Rozan, T.F., Rickard, D., Rowlands, C.C. & Oldroyd, A. (2002) Aqueous copper sulfide clusters as intermediates during copper sulfide formation. *Environ. Sci. Technol.* 36, 394–402.
- McKibben, M.A. & Barnes, H.L. (1986) Oxidation of pyrite in low temperature acidic solutions – rate laws and surface textures. *Geochim Cosmochim Acta*, 50, 1509-1520.
- Mullin, J.W. (2011) *Crystallization*, 4th Ed. Butterworth-Heinemann, 600 p.
- Nordstrom, D.K. (1982) The effect of sulfate on aluminum concentrations in natural waters: some stability relations in the system Al₂O₃-SO₃-H₂O at 298 K. *Geochim. Cosmochim. Acta* 46, 681-692.
- Nordstrom, D.K. (1985) The rate of ferrous iron oxidation in a stream receiving acid mine effluent. *Selected papers in the hydrologic sciences. US Geological Survey Water Supply Paper* 113-119.
- Nordstrom, D.K. (2008) *Questa baseline and pre-mining ground-water quality investigation*, 25. Summary of results and baseline and pre-mining ground-water geochemistry, Red River Valley, Taos County, New Mexico, 2001-2005. *US Geological Survey Professional Paper* 1728, 111 p.
- Nordstrom, D.K. & Ball, J.W. (1986) The geochemical behavior of aluminum in acidified surface waters. *Science* 232, 54-56.
- Nordstrom, D.K., & Alpers, C.N. (1999a) *Geochemistry of acid mine waters*. In: Plumlee, G.S. & Logsdon, M.J. (eds.), *The Environmental Geochemistry of Mineral Deposits, Part A. Processes, Techniques, and Health Issues: Society of Economic Geologists, Rev. Econ. Geology* 6A, 133-156.
- Nordstrom, D.K. & Alpers, C.N. (1999b) Negative pH, efflorescent mineralogy, and consequences for environmental restoration at the Iron Mountain Superfund site, California. *Proc. Natl. Acad. Sci.*, 96, 3455-3462.
- Nordstrom, D.K., Ptacek, C.J. & Blowes, D.W. (2000) Negative pH and extremely acidic mine waters from Iron Mountain, California. *Environ Sci Technol*, 34, 254-258.
- Nordstrom, D.K. & Archer, D. (2003) Arsenic thermodynamic data and environmental geochemistry. In Welch, A. & Stollenwerk, K. (Eds.), *Arsenic in Ground Water*, Kluwer Publisher, pp. 1–26.
- Patrick, R.A.D., Mosselmans, J.F.W., Charnock, J.M., England, K.E.R., Helz, G.R., Garner, C.D. & Vaughan, D.J. (1997) The structure of amorphous copper sulfide precipitates: An X-ray absorption study. *Geochim. Cosmochim. Acta* 61, 2023–2036.
- Pitzer, K.S. (1986) Theoretical considerations of solubility with emphasis on mixed aqueous electrolytes. *Pure App Chem*, 58-12, 1599-1610
- Plummer, L.N., Parkhurst, D.L., Fleming, G.W. & Dunkie, S.A (1988) A computer program incorporating Pitzer's equations for calculation of geochemical reactions in brines. *U.S. Geol. Survey, Water-Resources Investigations Report* 88-4153, Reston, Virginia.
- Postgate, J.R. (1984) *The sulfate-reducing bacteria*, second. ed. Cambridge University Press, Cambridge, UK.
- Regenspurg, S., Brand, A. & Peiffer, S. (2004) Formation and stability of schwertmannite in acidic mining lakes. *Geochim. Cosmochim. Acta*, 68-6, 1185-1197.
- Ritchie, A.I.M. (2003) Oxidation and gas transport in piles of sulphidic material. (In Jambor, J.L. Blowes, D.W. & Ritchie A.I.M., Eds.) *Environmental Aspects of Mine wastes, Mineralogical Association of Canada, Short Course Series Volume* 31 (R Raeside, ed.), pp. 73-94, Vancouver, British Columbia.)
- Sánchez-España, J. (2007) *The behavior of iron and alu-*

- minum in acid mine drainage: Speciation, Mineralogy, and Environmental Significance. In T.M. Letcher (ed.), *Thermodynamics, Solubility and Environmental Issues*, Elsevier B.V., The Netherlands, pp. 137-149.
- Sánchez-España, J. & Yusta, I. (2015) Low-crystallinity products of trace metal precipitation in neutralized pit-lake waters without ferric and aluminous adsorbent: Geochemical modelling and mineralogical analysis. *Mineralogical Magazine* 79(3), 781-798.
- Sánchez-España, J., López-Pamo, E. & Santofimia, E. (2007a) The oxidation of ferrous iron in acidic mine effluents from the Iberian Pyrite Belt (Odiel Basin, Huelva, Spain): Field and laboratory rates. *Journal of Geochemical Exploration* 92, 120-132.
- Sánchez-España J., Santofimia E. & López-Pamo E. (2007b) Iron terraces in acid mine drainage systems: A discussion about the organic and inorganic factors involved in their formation through observations from the Tintillo acidic river (Riotinto mine, Huelva, Spain). *Geosphere* 3(3), 133-151.
- Sánchez-España, J., López Pamo, E., Santofimia, E., Aduvire, O., Reyes, J. & Barettino, D. (2005) Acid Mine Drainage in the Iberian Pyrite Belt (Odiel river watershed, Huelva, SW Spain): Geochemistry, Mineralogy and Environmental Implications. *Applied Geochemistry* 20-7, 1320-1356.
- Sánchez-España, J., López-Pamo, E., Santofimia, E., Reyes, J. & Martín Rubí, J.A. (2006) The removal of dissolved metals by hydroxysulfate precipitates during oxidation and neutralization of acid mine waters, Iberian Pyrite Belt. *Aquat Geochem* 12, 269-298.
- Sánchez-España, J. & Diez Ercilla, M. (2008) Geochemical modelling of concentrated mine waters: A comparison of the Pitzer ion-interaction theory with the ion-association model for the study of melanterite solubility in San Telmo mine (Huelva, Spain). In Stefánsson O. (Ed.), *Geochemistry Research Advances*, Nova Science Publishers, New York, p. 31-55.
- Sánchez-España, J., Diez Ercilla, M., González Toril, E., López-Pamo, E., Santofimia Pastor, E., San Martín-Úriz, P. & Amils, R. (2008) Biogeochemistry of a hyperacidic and ultraconcentrated pyrite leachate in San Telmo (Iberian Pyrite Belt, Spain). *Water, Air and Soil Pollution*, 194, 243-257.
- Sánchez-España J., Yusta I. & Diez M. (2011) Schwertmannite and hydrobasaluminite: A re-evaluation of their solubility and control on the iron and aluminum concentration in acidic pit lakes. *Applied Geochemistry* 26, 1752-1774.
- Sánchez-España, J., Yusta, I. & López, G. A. (2012) Schwertmannite to jarosite conversion in the water column of an acidic mine pit lake. *Mineral. Mag.* 76, 2659-2682.
- Sánchez-España, J., Boehrer, B. & Yusta, I. (2014) Extreme carbon dioxide concentration in acidic pit lakes provoked by water/rock interaction. *Environ. Sci. Technol.* 48(8), 4273-4281.
- Sánchez-España, J., Yusta, I., Gray, J. & Burgos, W.D. (2016a) Geochemistry of dissolved aluminum at low pH: Extent and significance of Al-Fe(III) coprecipitation below pH 4.0. *Geochim Cosmochim Acta*, 175, 128-149.
- Sánchez-España, J., Yusta, I. & Burgos, W.D. (2016b) The geochemistry of dissolved aluminum at low pH: Hydrobasaluminite formation and interaction with silica, trace metals and microbial cells under anoxic conditions. *Chemical Geology* 192, 70-96.
- Singer, P.C. & Stumm, W. (1970) Acidic mine drainage: the rate-determining step. *Science*, 167, 1121-1123.
- Stoffregen, R.E., Alpers, C.N. & Jambor, J.L. (2000) Alunite-Jarosite crystallography, thermodynamics, and geochronology. In *Sulfate Minerals: Crystallography, Geochemistry, and Environmental Significance* (Alpers, C.N., Jambor, J.L., Nordstrom, D.K., Eds.). *Reviews in Mineralogy & Geochemistry*, 40, 453-479.
- Stumm, W. & Morgan, J.J. (1996) *Aquatic chemistry*, 3th ed. John Wiley & Sons, New York.
- Tavare, N.S. (1995) *Industrial crystallization*. Plenum Press, New York.
- Velasco, F., Alvaro, A., Suarez, S., Herrero, M. & Yusta, I. (2005) Mapping Fe-bearing hydrated sulfate minerals with short wave infrared (SWIR) spectral analysis at San Miguel mine environment, Iberian Pyrite Belt (SW Spain). *J. Geochem. Expl.*, 87-2, 45-72.
- Wendt-Potthoff, K., Koschorreck, M., Diez-Ercilla, M. & Sánchez-España, J. (2012) Microbial activity and biogeochemical cycling in a nutrient-rich meromictic acid pit lake. *Limnologica - Ecology and Management of Inland Waters* 42(3), 175-188.
- Yang, C. H. & Qiu, H. (1986) Theory of homogeneous nucleation: A chemical kinetic view. *The Journal of Chemical Physics* 84, 416

Multi-step crystallization pathways in natural and engineered cements

/ Alejandro Fernandez-Martinez

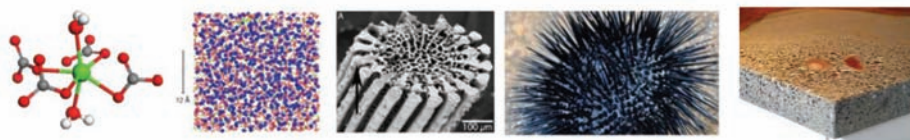
ISTerre, CNRS & Univ. Grenoble Alpes, 38041 Grenoble Cedex, France

1. Introduction

A cement is a material with binding properties that hold together the different components of structures such as bridges, buildings and monuments. Engineered cements have been produced for centuries now, mostly from the calcination and melting of limestone and aluminosilicates. Ordinary Portland cement (OPC), is actually the most produced material in the world, with more than 4,000 million metric tons per year. Cement hydration involves a combination of dissolution and re-precipitation processes through which a variety of hydrated phases are formed. Calcium silicate hydrates (C-S-H, using the cement notation), are the most abundant family of binders. They have a complex, non-uniform stoichiometry (varying Ca/Si ratios and water content) and nanocrystalline character. C-S-H is the main phase in OPC, responsible for its strength and durability. Other engineered cements include for instance basanite ($\text{CaSO}_4 \cdot 0.5\text{H}_2\text{O}$, plaster of Paris), portlandite ($\text{Ca}(\text{OH})_2$) and geopolymers. The latter are a kind of supplementary cementitious materials (SCM_s) that are used in combination with OPC to decrease the CO₂ footprint from OPC production. OPC production accounts for 5–7% of the global human-made CO₂ emissions, posing a technological challenge in the search for ‘green’ OPC replacements.

In spite of the extensive use of engineered cements and the development of new families of SCMs to improve workability, setting rate and to lower the cement CO₂ footprint, many aspects of the initial steps of the cement hydration process remain unknown, including the mechanisms of C-S-H nucleation (*Garrault-Gauffinet & Nonat, 1999*). Moreover, the physico-chemical conditions under which cement hydrates form are extreme, such as the high alkalinity (cement pore water pH values of 13) and their crystallization in restricted, confined spaces. These are important points that hamper our ability to direct cement nucleation, for instance, for the restoration of cultural heritage or for healing of fractures and pores in engineered structures.

An analogy to cement materials can be made with the ‘natural binders’ that compose multiple structures such as our teeth, marine shells and bones, forming natural (nano) composites. These ‘natural cements’ are widespread, fundamental components of living organisms that offer them physical and chemical protection and articulate them (*Rieger et al., 2014*). These include, to name a few examples, the apatite formed in the nanopores between collagen fibers of our teeth, the aragonite tablets in the nacre shells or the calcite that forms the spicules of the sea urchin (*Addadi et al., 2003*). Biominerals are a clear example of directed mineral precipitation allowing functional development. Crystallization of biominerals is dictated by a complex interplay of organic and inorganic additives and external ‘biological substrates’ that direct the nucleation through multiple steps, allowing the controlled precipitation of a mineral phase at specific location, typically in a confined space, and at a given time. They offer a perfect benchmark from which to improve the development of our cement technology.



2. Multi-step crystallization pathways

In recent years, complex multi-stage nucleation pathways have been reported for iron oxides, carbonate, phosphate and sulfate minerals. These so-called non-classical pathways include the formation of stable or kinetically trapped aqueous species that act as precursors of the final crystalline polymorphs (Benzerara *et al.*, 2014; Gebauer *et al.*, 2008; Wallace *et al.*, 2013) (see Fig. 1). Pre-nucleation clusters (PNCs) (Gebauer *et al.*, 2008), polymer-induced liquid precursors (PILP) (Gower & Odom, 2000), or dynamically ordered liquid like oxyanion polymers (DOLLOP) (Demichelis *et al.*, 2011), are examples of aqueous precursor species reported for the CaCO_3 system. These precursor species have been shown to aggregate in solution, forming amorphous calcium carbonate (ACC), an amorphous material that subsequently crystallizes as a CaCO_3 polymorph. Amorphous precipitates have been also reported for the phosphate system, forming as well from aqueous clusters. These aqueous species and amorphous precursors offer ‘shortcuts’ throughout the free energy landscape for the formation of crystalline polymorphs, supposedly decreasing the interfacial free energies and consequently lowering the barrier(s) to nucleation (Navrotsky, 2004). This contrasts with the ‘classical view’ of a crystal growth process via ion-by-ion addition. A prototypical example in the field of biomineralization is that of the sea-urchin (Politi *et al.*, 2008). At the early stages of development, sea urchin spicules are made out of ACC that crystallizes into calcite at later stages. The moldable hydrated structure of ACC procures that the sea urchin, among other organisms, can create the intricated shapes of their shells and/or skeletons, acting as a very effective cement, with pore-filling character (Yang *et al.*, 2011).

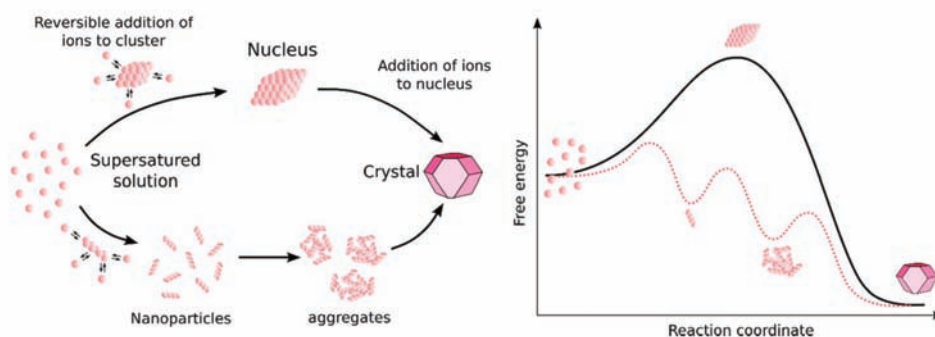


Fig. 1. Classical (top arrow) and so-called ‘non-classical’ (bottom arrow) nucleation pathways through the formation of nanoparticles, aggregates (amorphous intermediates), and a schematic energetic landscape. Adapted from (Sleutel & Van Driessche, 2014).

Biomimicry: enabling new cement technologies

The discovery of the PILP intermediate by L. Gower in the early 2000s (Gower, 2008; Gower & Odom, 2000) started a slow-developing revolution in the way mineral precipitation processes were and are used for engineered applications. Specifically, the so-called PILP process, i.e., the occurrence of a liquid-liquid separation in CaCO_3 , was reported also for apatite, opening the way for the development of dental remineralization strategies based on the same principle: the kinetic stabilization of a liquid polymer-like mineral (apatite) precursor that is able to diffuse within the pores of the (collagen) matrix, directing crystallization into the internal pores (Burwell *et al.*, 2012). This technology is a paradigmatic example of biomimicry, with high potential for many other applications in the cement industry.

In spite of all these advances, there are still fundamental questions that remain open about (i) the structure of the aqueous clusters leading to the formation of the amorphous / liquid-like precursors, and (ii) the specific factors that control the stability of these precursors,

their dehydration, and their further crystallization into crystalline polymorphs. In addition, the physico-chemical parameters controlling polymorph selections mechanism remain unknown. Some authors have proposed that water plays an important role as stabilizer of the amorphous structure (Raiteri & Gale, 2010) in the CaCO_3 system. At the same time, it is known that non-collagenous proteins and inorganic ions are present naturally occurring crystallization intermediates, but their roles in the stability and crystallization processes are still unknown (Addadi et al., 2003; Ihli et al., 2013). More research in these fields will enable the next generation of 'cement' products inspired by nature.

Engineered cements

Calcium silicate hydrate (C-S-H) is the most important binding phase in ordinary Portland cement. It forms as a result of a dissolution-precipitation process involving highly reactive clinker materials. C-S-H is by nature poorly crystalline, with an atomic structure similar to that of a disordered tobermorite, including turbostratic disorder and the presence of $\text{Ca}(\text{OH})_2$ sheets at high Ca/Si values. The formation process of C-S-H is therefore dominated by nucleation, with only limited growth. Whereas many studies have focused on the mesoscale structural evolution of the process of cement hydration only a few studies have addressed the formation mechanisms of C-S-H in detail (Bligh et al., 2016; Garrault-Gauffinet & Nonat, 1999). Garrault-Gauffinet & Nonat (1999) used changes in electrical conductivity to follow C-S-H formation, and interpreted their results using classical nucleation theory (CNT). Whereas their results are self-consistent within the framework of CNT, the lack of physical and chemical characterization of the initial precipitates renders their claim of CNT little credibility. Indeed, the recent advances in the understanding of carbonate formation processes have taught us about the need for in situ characterization of the early stages. A recent study on C-S-H nucleation has brought into light the existence of a Si-rich amorphous precursor to C-S-H. However, its structural and dynamical characteristics, as well as its chemical composition

and its transformation to C-S-H remain elusive as of today (Krautwurst et al., 2017). Work remains to be done in order to put in perspective the importance of this amorphous precursor to C-S-H.

3. Crystallization under confinement

Nucleation phenomena in engineered and natural cements take place often in micro- or nanoscopic pores. Understanding the factors that control nucleation and growth of solid phases in porous media, and how they differ from the bulk, is still an ongoing task. The reason is related to the different levels of complexity related to the problem. These include: (i) the lack of a unified picture of water structure, dynamics and energetics in confined spaces; (ii) a poor understanding of ion speciation in confinement and under reduced water activity; and (iii) a lack of knowledge about the interplay of the different factors controlling nucleation (pore controlled solubility vs. interfacial chemistry). Points (i) and (ii) are not treated here. A wide array of literature exists regarding these issues. Moreover, the development of advanced scattering, spectroscopic and imaging techniques, as well as computer simulation, is advancing these questions at significant pace. The point (iii), related to the nucleation process under confinement itself, has been addressed by different authors over the last three decades. Some of the main ideas are discussed here.

Pore-size controlled solubility effects

A pore-size control on the solubility of crystals growing in confined pores has been widely reported (Flatt, 2002; Scherer, 1999). This phenomenon, called the 'Pore-size Controlled Solubility' effect (PCS), comes from the fact that an extra energetic term is present for highly curved (small) crystals growing in confinement. It is explained by classical thermodynamics. According to the Young-Laplace equation, the pressure difference, Δp , across a solid-liquid interface is proportional to the curvature of the interface, with the interfacial tension being the proportionality constant. A complete thermodynamic treatment of this effect is described in Scherer (2002). This excess pressure shifts

the solubility of the crystal from the bulk solubility S_0 to an effective solubility S_d . For a crystal forming in a cylindrical pore this can be expressed as:

$$\frac{S_d}{S_0} = \exp\left(\frac{-\Delta p v}{nRT}\right) = \exp\left(\frac{-v}{nRT} \frac{2\gamma \cos\theta}{d}\right)$$

[equation 1]

where v is the molar volume of the crystallizing solute, T is the absolute temperature, R is the ideal-gas constant, n is the number of moles crystallizing, d is the pore diameter and θ is the contact angle between the growing crystal and the pore surface. PCS effects have been also incorporated recently to reactive transport models that account for the observed cementation of large pores during fluid transport through a heterogeneous rock matrix (Emmanuel *et al.*, 2007; Emmanuel & Ague, 2009). Plots of S_d/S_0 values are shown in Fig. 2, as a function of pore size, d , and of the interfacial free energy of the growing cluster/water interface, (Emmanuel & Ague, 2009).

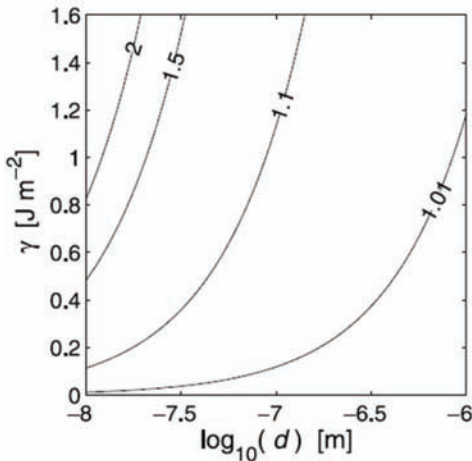


Fig. 2. Plot of the effective saturation (S_d/S_0) as a function of pore size, d , and interfacial energy, γ , for a crystal growing in a cylindrical pore. Calculated from eq. 1 using values in Table 1 with $T = 373$ K. From (Emmanuel & Ague, 2009).

It is interesting to see that the pore-size effect can be considered as negligible in cases where the interfacial free energy is relatively low. For instance, solid/water interfacial free energies for the most common

crystallographic faces of gypsum and calcite (two widely used minerals in cement applications) are in the order of $\gamma_{\text{CaSO}_4} = 0.01$ J/m² and $\gamma_{\text{CaCO}_3} = 0.1$ J/m². This makes that, in the whole range of pore sizes, from the micron to the nanoscale, the enhancement of the supersaturation is not expected to exceed a 10%, i.e., $S_d/S_0 < 1.1$.

Kinetic effects

A seminal paper in this field was published by (Prieto *et al.*, 1990). These authors observed that the supersaturation attained by salts nucleating in gel pores was proportional to the increase rate of the supersaturation itself. They introduced the concept of ‘threshold supersaturation’ (Prieto *et al.*, 1990; Putnis *et al.*, 1995) meaning the supersaturation that has to be attained to spark crystallization at a given supersaturation rate. Note that this is a kinetic concept, defined after non-equilibrium experiments with solution supersaturation values evolving in time. The experiments were performed using a porous medium consisting of a column with a silica aerogel, with pores in the range 2 – 200 nm. The system is feeded with an anionic and a cationic solution, one arriving from each side. This geometry yields a non-uniform distribution of solution supersaturation values along the column that evolves with time. An empirical law relating supersaturation rate (q) and threshold supersaturation (σ) was proposed (see Fig. 3):

$$q = k\sigma_t^m \quad (\text{equation 2})$$

where k and m are a proportionality constant and an exponent respectively. This empirical law applies also in the case of supercooled solutions (supercooling: lowering the temperature of a liquid below its freezing point without it becoming a solid). Studies over the last few decades have shown that undercooling ΔT ($\Delta T = T_{\text{freeze}} - T_{\text{cryst}}$) is maximized in confinement and by increasing solution cooling rates (Kashchiev *et al.*, 2010). Whether the supersaturation is attained by cooling or by increasing the concentration of a salt in a solution this law is of general applicability. The exponent m and the proportionality constant depend then on the nature of the nucle-

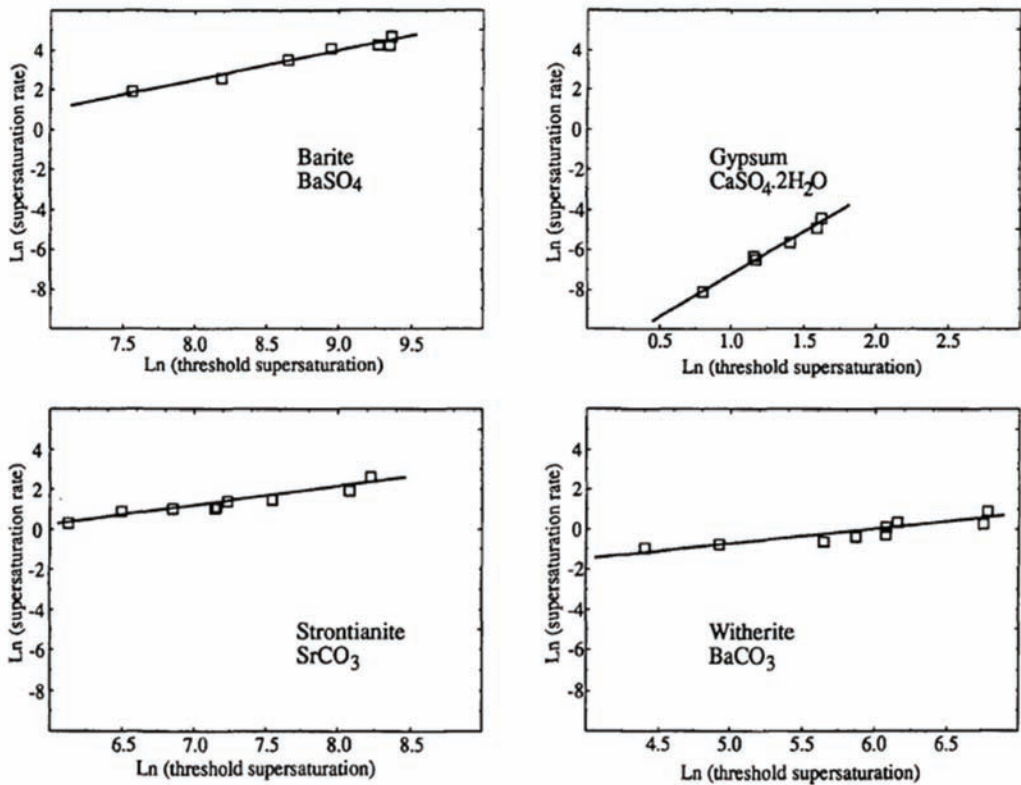


Fig. 3. Plots of the supersaturation rate as a function of the threshold supersaturation for barite, gypsum, strontianite and witherite. From (Putnis et al., 1995).

ated solid, on the volume (confinement) and on the thermal history of the solution.

The explanations to these phenomena were attributed to kinetic effects related with the limited supply of growth units to a growing nucleus in a nanopore. Restricted dynamics of aqueous solutions in confined media have been reported to occur in nanopores filled with CaCl_2 and LiCl (Mamontov et al., 2008). Interestingly, the greatest suppression of water dynamics is found for CaCl_2 solutions, indicating that there may be a collaborative effect of cation charge, hydration environment and confinement geometry. More studies on this field are needed to understand what are the limiting mechanisms for solute transport, and the influence of pore surface chemistry.

Surface chemistry

Confinement also influences pore surface chemical properties, potentially impacting heterogeneous nucleation phenomena. (Wang et al., 2003) have shown that the acidity constants (pK_{a1} and pK_{a2}) of functional groups in mesoporous alumina are shifted with respect to those of a bulk alumina, the porous material having neutral charge over a narrower range of pH. This gives rise to a high surface charge density in mesoporous materials, which influences their ion adsorption edges enhancing ion adsorption. Similarly, convex curved surfaces have been reported to shift acidity constants of functional groups on the external surface of imogolite nanotubes with respect to those of gibbsite (its planar counterpart) (Fernandez-Martinez, 2009).

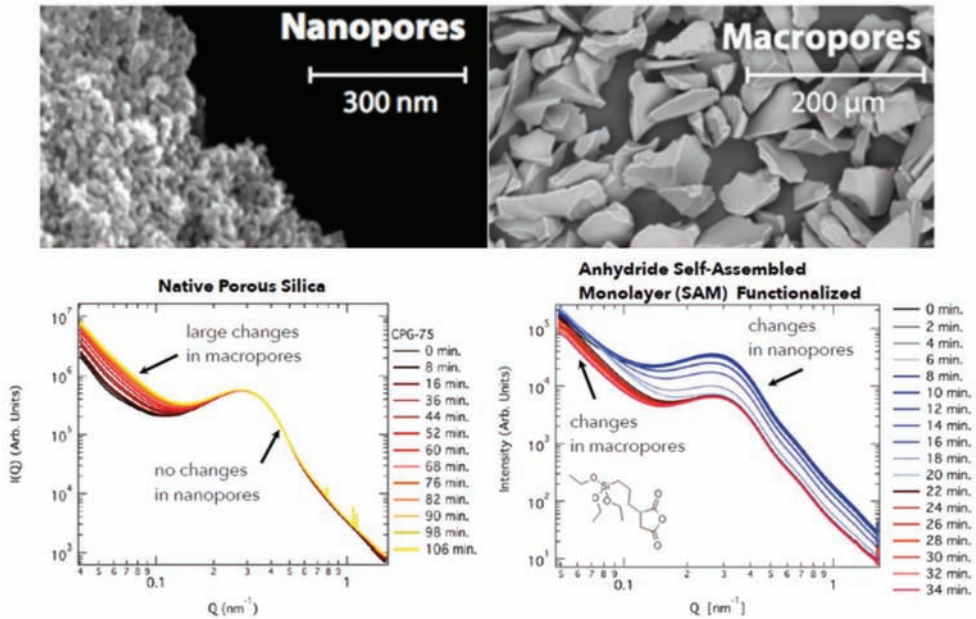


Fig. 4. Top: SEM image of the mesoporous silica material (CPG-75) used in the Small-Angle X-ray Scattering (SAXS) experiments, showing the nanopores and macropores. Bottom: SAXS patterns taken during the in-situ CaCO_3 precipitation experiment. The left graph shows an increase in the intensity at low angle with time, indicating precipitation in the raw SiO_2 macropores. The right graph shows changes in the intensity at the nanopore scale, as a result of CaCO_3 precipitation in the carboxyl-terminated silica material. Modified from Stack et al., (2014).

Whereas the inhibition of mineral nucleation in nanopores has been explained successfully by the PCS effect in many cases (Emmanuel et al., 2007; Emmanuel & Ague, 2009; Putnis & Mauthe, 2001), recent observations suggest that the PCS effect is not dominant in cases where surface chemistry offers a preferential template for mineral nucleation (Stack et al., 2014). This hypothesis has been recently reinforced by statistical physics models of heterogeneous nucleation (Hedges and Whitlam, 2013). Indeed, Stack et al. (2014) showed that CaCO_3 nucleated preferentially in nanopores functionalized with carboxyl-terminated organic moieties that offered a good template for precipitation (Fig. 4). ACC was determined to be the nucleated form of CaCO_3 . Interestingly, ACC has been shown to be stabilized under confinement (Stephens et al., 2010). This fact points to confinement as a hypothetic important parameter controlling CaCO_3 nucleation in biominerals, and governing the crystallization kinetics of

PILP or amorphous intermediates. These results highlight the need for further investigations in order to develop consistent thermodynamic models of precipitation phenomena at the nanoscale.

4. Conclusions and perspectives

Studies addressing nucleation and growth of biominerals have significantly impacted our understanding of the fundamental mechanisms underlying these complex phenomena. The discovery of multi-step nucleation processes and of aqueous intermediates to nucleation, together with the phase separation occurring in the liquid state of highly supersaturated solutions, opens new perspectives for the development of biomimetic materials, especially in the field of engineered materials. However, significant gaps remain present in our knowledge of fundamental processes. These include the applicability of classical nucleation theory to these multi-step nucleation pathways, or the numerous physico-chemical factors affecting nucle-

ation in confined spaces.

A feedback between our studies on natural and engineered systems is necessary. Recent studies on C-S-H nucleation have brought into light the existence of an amorphous precursor to C-S-H. Determining the crystallization pathway is of special relevance for the development of effective cement retardants and for the chemical industry: the potential occurrence of aggregation-based processes of the initially formed amorphous 'droplets' (i.e., a physical process) would open new possibilities for the stabilization of these C-S-H precursors.

References

- Addadi, L., Raz, S. & Weiner, S. (2003) Taking advantage of disorder: Amorphous calcium carbonate and its roles in biomineralization. *Adv. Mater.* 15, 959–970. doi:10.1002/adma.200300381
- Benzerara, K., Skouri-Panet, F., Li, J., Féraud, C., Gugger, M., Laurent, T., Couradeau, E., Ragon, M., Cosmidis, J., Menguy, N., Margaret-Oliver, I., Tavera, R., López-García, P. & Moreira, D. (2014) Intracellular Ca-carbonate biomineralization is widespread in cyanobacteria. *Proc. Natl. Acad. Sci. U. S. A.* 111, 10933–8. doi:10.1073/pnas.1403510111
- Bligh, M.W., d'Eurydice, M.N., Lloyd, R.R., Arns, C.H. & Waite, T.D. (2016) Investigation of early hydration dynamics and microstructural development in ordinary Portland cement using ¹H NMR relaxometry and isothermal calorimetry. *Cem. Concr. Res.* 83, 131–139. doi:10.1016/j.cemconres.2016.01.007
- Burwell, A.K., Thula-Mata, T., Gower, L.B., Habeliz, S., Kurylo, M., Ho, S.P., Chien, Y.-C., Cheng, J., Cheng, N.F., Gansky, S.A., Marshall, S.J. & Marshall, G.W. (2012) Functional Remineralization of Dentin Lesions Using Polymer-Induced Liquid-Precursor Process. *PLoS One* 7, e38852. doi:10.1371/journal.pone.0038852
- Demichelis, R., Raiteri, P., Gale, J.D., Quigley, D. & Gebauer, D. (2011) Stable prenucleation mineral clusters are liquid-like ionic polymers. *Nat. Commun.* 2, 590.
- Emmanuel, S. & Ague, J.J. (2009) Modeling the impact of nano-pores on mineralization in sedimentary rocks. *Water Resour. Res.* 45.
- Emmanuel, S., Ague, J.J. & Berkowitz, B. (2007) Reactive transport and pore-size controlled solubility in porous rocks. *Geochim. Cosmochim. Acta* 71, A255–A255.
- Fernandez-Martinez, A., (2009) Physics of natural nanoparticles – water interfaces: chemical reactivity and environmental implications. *Ec. Dr. Terre, Univers Environ. Universite Joseph-Fourier, Grenoble (France)*.
- Flatt, R.J. (2002) Salt damage in porous materials: how high supersaturations are generated. *J. Cryst. Growth* 242, 435–454.
- Garrault-Gauffinet, S. & Nonat, A. (1999) Experimental investigation of calcium silicate hydrate (C-S-H) nucleation. *J. Cryst. Growth* 200, 565–574. doi:10.1016/S0022-0248(99)00051-2
- Gebauer, D., Volkel, A. & Colfen, H. (2008) Stable prenucleation calcium carbonate clusters. *Science* (80-.). 322, 1819–1822. doi:10.1126/science.1164271
- Gower, L.B. (2008) Biomimetic model systems for investigating the amorphous precursor pathway and its role in biomineralization. *Chem. Rev.* 108, 4551–627. doi:10.1021/cr800443h
- Gower, L.B. & Odom, D.J. (2000) Deposition of calcium carbonate films by a polymer-induced liquid-precursor (PILP) process. *J. Cryst. Growth* 210, 719–734. doi:10.1016/S0022-0248(99)00749-6
- Hedges, L.O. & Whitelam, S. (2013) Selective nucleation in porous media. *Soft Matter* 9, 9763. doi:10.1039/c3sm51946e
- Ihli, J., Kim, Y.-Y., Noel, E.H. & Meldrum, F.C. (2013) The Effect of Additives on Amorphous Calcium Carbonate (ACC): Janus Behavior in Solution and the Solid State. *Adv. Funct. Mater.* 23, 1575–1585. doi:10.1002/adfm.201201805
- Kashchiev, D., Borissova, A., Hammond, R.B. & Roberts, K.J. (2010) Effect of cooling rate on the critical undercooling for crystallization.

- J. Cryst. Growth 312, 698–704. doi:10.1016/j.jcrysgro.2009.12.031
- Krautwurst, N., Nicoleau, L., Dietzsch, M., Lieberwirth, I., Labbez, C., Fernandez-Martinez, A., Driessche, A. van, Barton, B., Leukel, S. & Tremel, W. (2017) Two-Step Nucleation Process of Calcium Silicate Hydrate, the Nano-Brick of Cement. Submitted.
- Mamontov, E., Cole, D.R., Dai, S., Pawel, M.D., Liang, C.D., Jenkins, T., Gasparovic, G. & Kintzel, E. (2008) Dynamics of water in LiCl and CaCl₂ aqueous solutions confined in silica matrices: A backscattering neutron spectroscopy study. Chem. Phys. 352, 117–124. doi:10.1016/j.chemphys.2008.05.019
- Navrotsky, A. (2004) Energetic clues to pathways to biomineralization: Precursors, clusters, and nanoparticles. Proc. Natl. Acad. Sci. U. S. A. 101, 12096–12101. doi:10.1073/pnas.0404778101
- Politi, Y., Metzler, R.A., Abrecht, M., Gilbert, B., Wilt, F.H., Sagi, I., Addadi, L., Weiner, S. & Gilbert, P. (2008) Transformation mechanism of amorphous calcium carbonate into calcite in the sea urchin larval spicule. Proc. Natl. Acad. Sci. U. S. A. 105, 17362–17366. doi:10.1073/pnas.0806604105
- Prieto, M., Putnis, A. & Fernandez Diaz, L. (1990) Factors controlling the kinetics of crystallization - supersaturation evolution in a porous medium. Application to barite crystallization. Geol. Mag. 127, 485–495.
- Putnis, A. & Mauthe, G. (2001) The effect of pore size on cementation in porous rocks. Geofluids 1, 37–41.
- Putnis, A., Prieto, M. & Fernandez Diaz, L. (1995) Fluid supersaturation and crystallization in porous media. Geol. Mag. 132, 1–13.
- Raiteri, P. & Gale, J.D. (2010) Water is the key to nonclassical nucleation of amorphous calcium carbonate. J. Am. Chem. Soc. 132, 17623–34. doi:10.1021/ja108508k
- Rieger, J., Kellermeier, M. & Nicoleau, L. (2014) Formation of Nanoparticles and Nanostructures- An Industrial Perspective on CaCO₃, Cement, and Polymers. Angew. Chemie Int. Ed. 53, 2–19. doi:10.1002/anie.201402890
- Scherer, G.W. (1999) Crystallization in pores. Cem. Concr. Res. 29, 1347–1358.
- Sleutel, M. & Van Driessche, A.E.S. (2014) Role of clusters in nonclassical nucleation and growth of protein crystals. Proc. Natl. Acad. Sci. U. S. A. 111, E546-53. doi:10.1073/pnas.1309320111
- Stack, A.G., Fernandez-Martinez, A., Allard, L.F., Bañuelos, J.L., Rother, G., Anovitz, L.M., Cole, D.R. & Waychunas, G.A. (2014) Pore-Size-Dependent Calcium Carbonate Precipitation Controlled by Surface Chemistry. Environ. Sci. Technol. 48, 6177–6183. doi:10.1021/es405574a
- Stephens, C.J., Ladden, S.F., Meldrum, F.C. & Christenson, H.K. (2010) Amorphous Calcium Carbonate is Stabilized in Confinement. Adv. Funct. Mater. 20, 2108–2115.
- Wallace, A.F., Hedges, L.O., Fernandez-Martinez, A., Raiteri, P., Gale, J.D., Waychunas, G.A., Whitelam, S., Banfield, J.F. & De Yoreo, J.J. (2013) Microscopic evidence for liquid-liquid separation in supersaturated CaCO₃ solutions. Science (80-.). 341, 885–9. doi:10.1126/science.1230915
- Yang, L., Killian, C.E., Kunz, M., Tamura, N. & Gilbert, P.U.P.A. (2011) Biomineral nanoparticles are space-filling. Nanoscale 3, 603–9. doi:10.1039/c0nr00697a



Sociedad Española de Mineralogía
 Museo Geominero del Instituto Geológico
 y Minero de España
 c/ Calle de Ríos Rosas, 23
 28003 Madrid

SEM

organizadores:



patrocinadores:



Asturiana de Zinc, S.A.
 UNA COMPAÑIA GLENCORE

